2-1-2012

Reconfigurable filtenna for cognitive radio applications

Maria Elizabeth Zamudio

María Elizabeth Zamudio Moreno
Candidate

Electrical and Computer Engineering
Department

This thesis is approved, and it is acceptable in quality and form for publication:

Approved by the Thesis Committee:

Christos Christodoulou , Chairperson

Edl Schamiloglu

Joseph Costantine

RECONFIGURABLE FILTENNA FOR COGNITIVE RADIO APPLICATIONS

By

MARIA ELIZABETH ZAMUDIO MORENO

Electronic Technologists, Universidad Distrital Francisco José de Caldas, Bogotá- Colombia 2002

B.A., Telecommunications Engineer, Universidad Distrital Francisco José de Caldas, Bogotá- Colombia 2006

THESIS

Submitted in Partial Fulfillment of the
Requirements for the Degree of

Master of Science
Electrical Engineering

The University of New Mexico
Albuquerque, New Mexico

December 2011

DEDICATION

To my

Mother *and* Sister

With Love

ACKNOWLEDGMENTS

I would like to thank my family that is my support

I also thank my advisor dr. Christos Christodoulou, in whom I always find an inspiring positivism and enthusiasm.

Also my thanks to all the members of the antennas lab, they are also friends that make the research in the lab a good experience, specially I want to thank Dr Youssef Tawk

Additionally I thank to my friends that are always there to help me.

Finally I would like to thank the University of New Mexico Electrical and Computer Department for all their hard work and dedication.

RECONFIGURABLE FILTENNA FOR COGNITIVE RADIO APPLICATIONS

by

María Elizabeth Zamudio Moreno

Electronic Technologists, Universidad Distrital Francisco José De Caldas, Bogotá- Colombia 2002

B.A., Telecommunications Engineer, Universidad Distrital Francisco José de Caldas, Bogotá- Colombia 2006

M.S. Electrical Engineering, University of New Mexico, 2011

ABSTRACT

In order to improve the efficiency of the spectrum usage (available idle spectrum), cognitive radio devices should identify their environment, work in conjunction with other cognitive radio devices, and reconfigure themselves.

The concept that becomes crucial when designing cognitive radio devices is reconfigurability. Active components are used as switches in order to transform a device into a reconfigurable one. However, when switches are applied to an antenna design, we are not only making it reconfigurable, but we may also be affecting the electromagnetic properties of the reconfigurable communicating antenna. An alternate solution is presented in this thesis based on a

reconfigurable filter that is embedded in the feeding line of the cognitive antenna to produce a integrated antenna-filter combination which we call “Filtenna”

Two Filtenna designs are presented in this work. One of the designs is based on a band pass filter while the other utilizes a band reject filter. Furthermore, a varactor-based prototype was implemented and tested to provide the versatility required to tune a wideband Vivaldi antenna to a wide range of frequencies in a cognitive radio environment.

TABLE OF CONTENTS

LIST OF FIGURES

LIST OF TABLES

CHAPTER ONE

INTRODUCTION & MOTIVATION

The radio frequency spectrum has most of its allocations already assigned to licensed users; hence new alternative systems for RF utilization are arising. Cognitive Radio System (CR) is one of the possible alternative solutions since it proposes using the spectrum in a smarter way.

CR is based on the fact that the licensed users or primary users of the RF spectrum are not utilizing their spectral portion all the time; here the concept of secondary users appears. These users are able to use the channels that may become free when the primary users are not transmitting or receiving any data. Essentially, the system has to sense the wireless environment and based on this it detects when there is a free space to allow the secondary user to communicate.

To achieve the required functionality, a cognitive radio device must be able to follow a cycle of three functions as shown in figure 1.1. The first function is to **Sense** the RF environment. The second function is to **Act** which means sending the information when there is a communication opportunity. The last

function is to **Learn** from the environment in order to predict the parameters of the future communication based on the experience already obtained .

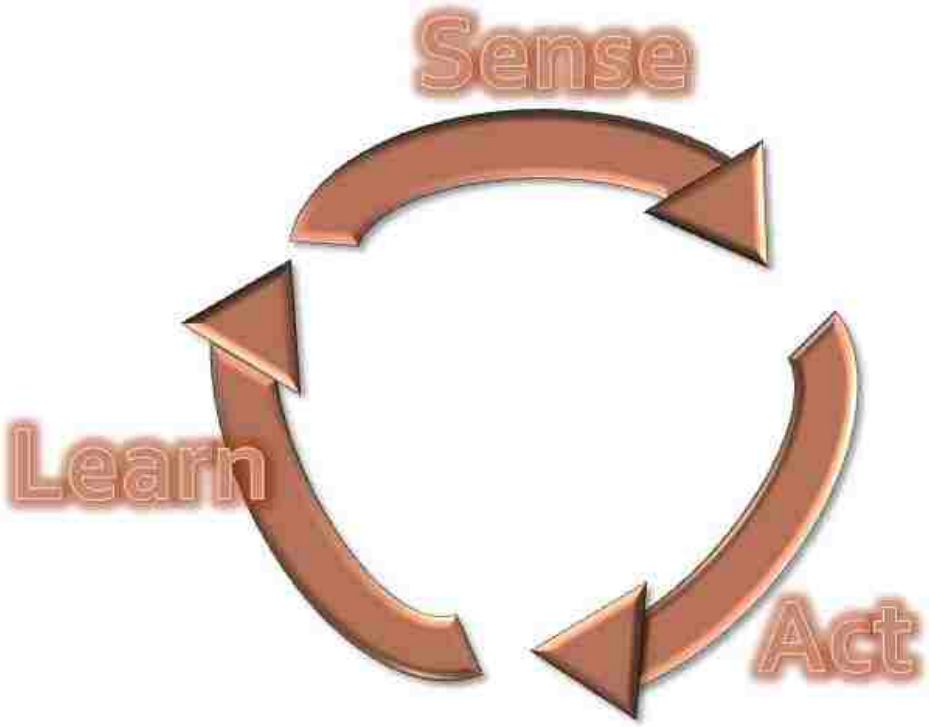

Figure 1.1: Cycle Flow for Cognitive Radio Devices

There is a need for antennas that can make a CR system work with other devices across multi-channels. The design of antennas for such systems is very challenging since it is expected to transmit at different frequencies and at different times. Therefore, reconfigurability becomes fundamental for a CR antenna.

Reconfigurability can be achieved by using active components (switches). To incorporate switches into an antenna structure, it is important to consider the activation/deactivation mechanism. For this purpose biasing lines should be

introduced into the design. However, if the biasing lines are not designed properly, they can alter the performance of the antenna since they can resonate and generate unwanted signals in the frequency of operation of the antenna.

An alternative is to integrate a reconfigurable filter within the antenna structure. The switches are added to the filter design thus avoiding adding any biasing lines in the radiating plane of the antenna. Such structure will be referred as “filtenna”.

The solution presented in this thesis is very practical and versatile for a CR system. The “filtenna” can allow or reject some frequency bands depending on the configuration of the filter.

.

CHAPTER TWO

COGNITIVE RADIO

Cognitive radio allows the introduction of secondary (unlicensed) users to the RF spectrum without affecting primary user's (licensed) communication. This is possible because primary users do not use their spectral space all the time. In November 2002, the FCC reported that 70% of the overall spectrum remains unemployed at any given time [2]. As a consequence, the FCC recommended alternatives to improve the spectrum usage. Three options were considered:

1-Spectrum reallocation which resulted in the opening of 700 MHz TV band for cognitive radio operation

2- Spectrum leasing that consists of an off-line solution were the licensed users can sell or trade their channels to third parties

3- Spectrum sharing where different solutions are suggested. These solutions are classified as either *underlay*, *overlay,* or *interweave* the signal of secondary users with the signal of primary users to minimize interference.

2.1. UNDERLAY

In the underlay technique both primary users and secondary users are allowed to transmit simultaneously as shown in figure 2.1. The secondary user

extends its signal over a large bandwidth to avoid overpassing the interference limits of the primary user. The interference constraints related with underlay systems make this technique useful only for short range communications. This technique is associated with Ultra Wide Band (UWB) spread spectrum as the modulation scheme.

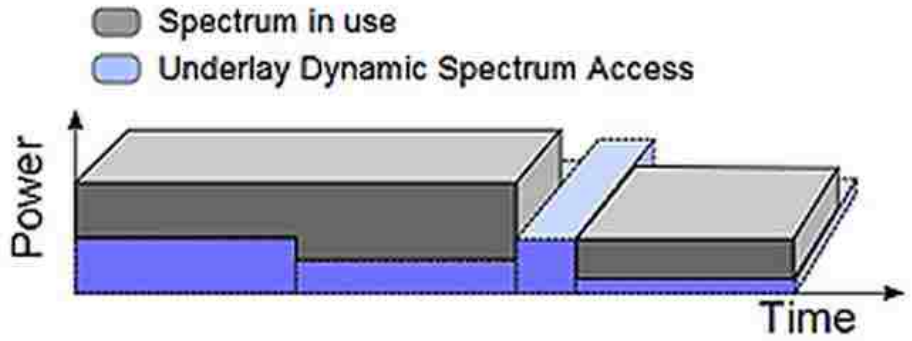

Figure 2.1:Underlay Technique [3]

2.2 OVERLAY

The overlay technique also allows simultaneous transmissions for the primary and secondary users as shown in figure 2.2. In this case the message of the primary user is prioritized over the message of the secondary user.

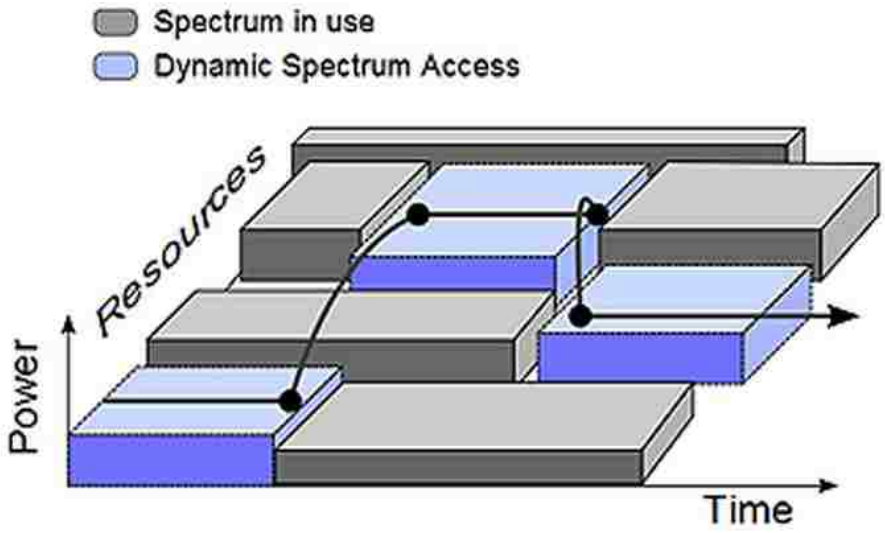

Figure 2.2: Overlay Technique [3]

The overlay technique uses two different strategies: The selfish approach, and selfless approach.

In the selfish approach, the secondary transmitter uses all the existing power to send its own message to the secondary receiver. Since the secondary user knows the primary user message, this information is used to cancel the interference caused to the primary user. In figure 2.3 a diagram for the selfish approach is shown where PT is the primary transmitter, ST is the secondary transmitter, PR is the secondary receiver and SR is the secondary receiver [6].

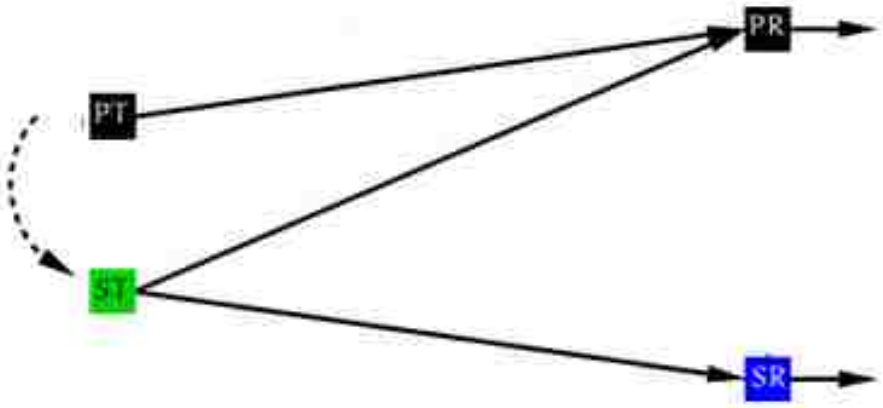

Figure 2.3: Selfish Approach Overlay Technique [6]

For the selfless approach, shown in figure 2.4, the secondary transmitter splits the power and uses part of it to retransmit the primary user message and the other part to send its own message. This split of power is selected such that the signal to noise rate (SNR) is balanced at the primary user. Consequently, the licensed user does not know the existence of the secondary user.

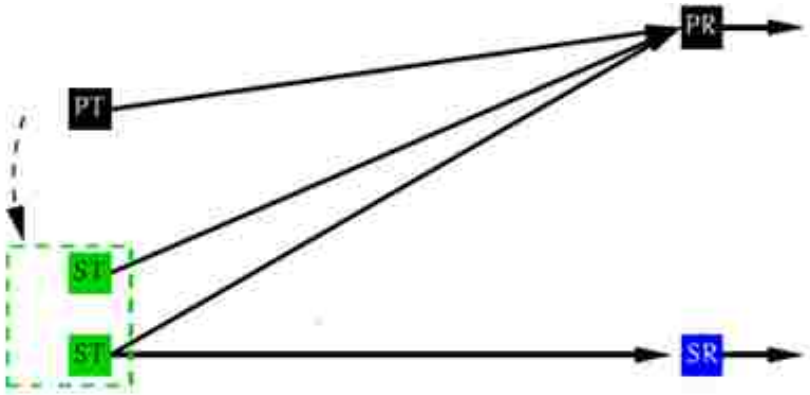

Figure 2.4: Selfless Approach Overlay Technique[6]

2.3 INTERWEAVE

In the interweave technique, the secondary user determines when and where to transmit by searching for spectral holes. These spectrum holes appear

when the primary user is not utilizing its channel. The spectrum holes change with geographic location, time and location in the spectrum. Therefore, the secondary user should monitor the radio spectrum constantly in order to detect the presence or the absence of licensed users in different frequency bands and then interweaves the secondary user signal through the holes that occur in different times and frequencies.

An interweave model is shown in figure 2.5 where there is a secondary Transmitter (ST), a secondary receiver (SR), and the primary users (PU) A, B and C. It is assumed that the secondary transmitter and the secondary receiver can detect primary transmissions perfectly within their respective sensing regions.

For this model the secondary transmitter detects spectral holes when both A and B are inactive; the cognitive receiver SR finds a communication opportunity when it detects that both B and C are inactive correspondingly.

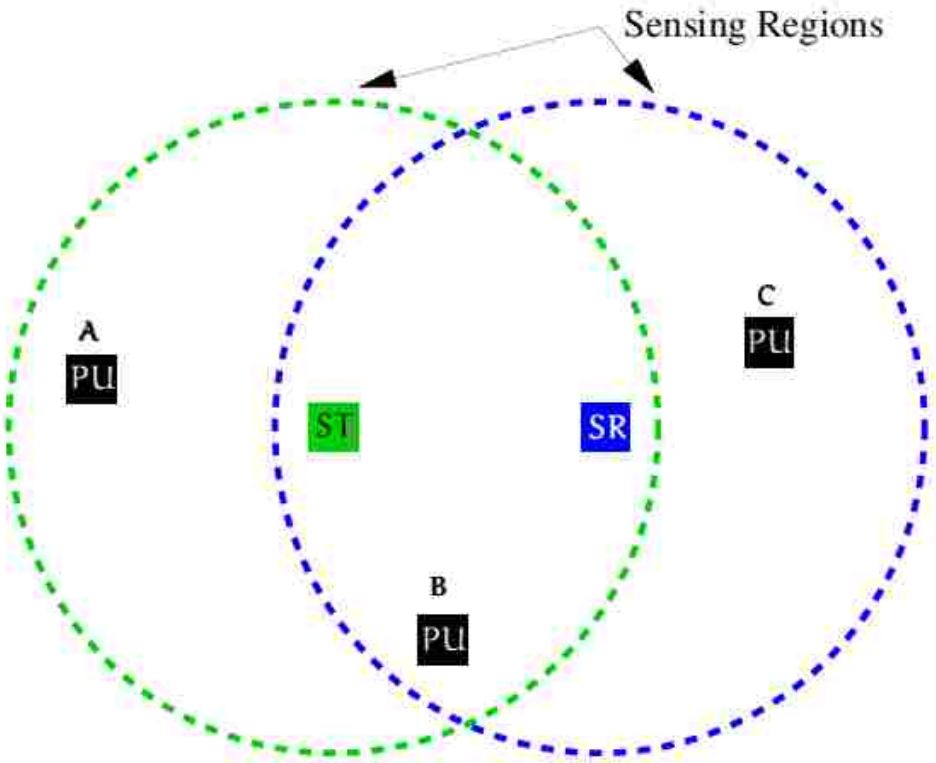

Figure 2.5: Conceptual Interweave Model [6]

2.5 Cognitive Radio Devices for Interweave and Underlay

Cognitive radio (CR) systems should be able to periodically sense gaps in the finite RF spectrum, which is already occupied by other wireless systems. Then the CR system should change its transmitter and receiver properties to be able to operate within the unoccupied detected channels.

The implementation of a CR system for the interweave model requires a sensing antenna that monitors continuously the wireless channels and detects the communication opportunities. The system also requires a reconfigurable antenna to transmit and receive data through the detected unused channels. The Implementation follows a CR chain as shown in figure 2.6.

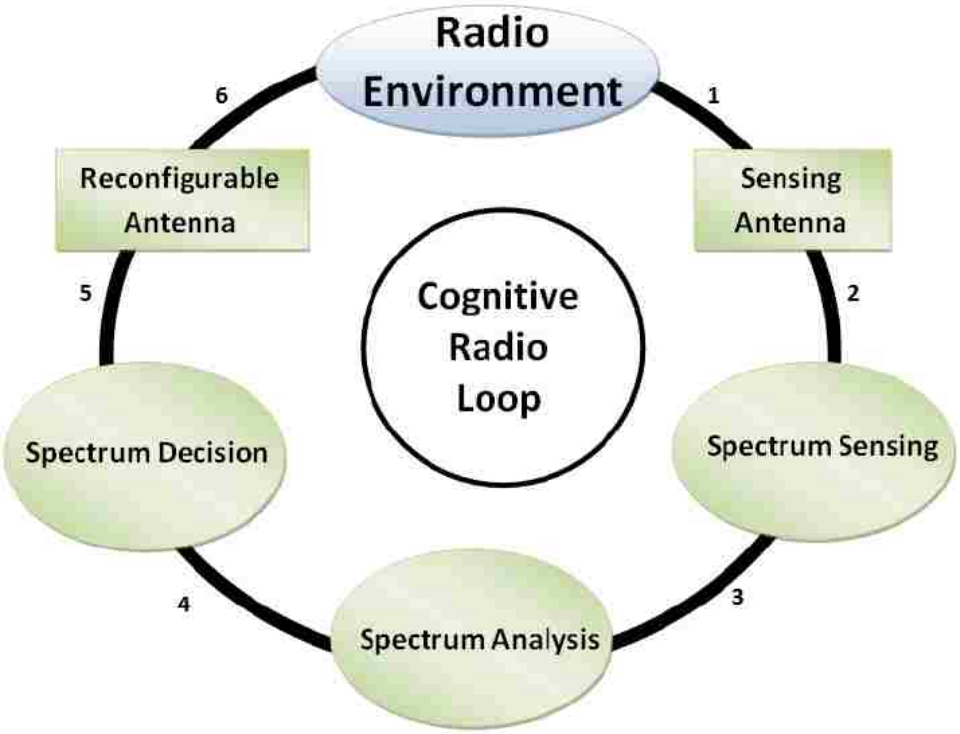

Figure 2.6: Cognitive Radio Chain [4]

Generally, the sensing antenna is a UWB antenna for channel sensing; while the reconfigurable antenna should have the capability to tune its operating frequency based on the primary user's activity in order to achieve communication. For the design of such system, three key parameters should be considered [5]:

1- The isolation between the two antenna ports: the operation of one of the antennas shouldn't be affected by the operation of the other antenna.

2- The dimension of the total antenna structure. The size should be optimized because the space used to accommodate both antennas should be as small as possible.
3- The radiation pattern for both antennas should be omni-directional. The antennas should be able to receive a signal at any given direction.

On the other hand, the implementation of a CR antenna system for the underlay model requires one port antenna where the antenna gives a UWB response with notches at the bands where the primary users are active. For the design of this kind of cognitive radio antenna system, three parameters should be considered [5]:

1- Reflection coefficient: Since the primary users operate at the notch frequency of the secondary users, the CR antenna system should be able to achieve a reflection coefficient close to 0 dB at its notch frequency.
2- Gain fluctuation: the variations in the antenna gain should be minimized.
3- Radiation pattern: the radiation pattern of the antenna should remain omni-directional over the whole UWB.

CHAPTER THREE

RECONFIGURABLE MICROWAVE FILTERS

This chapter discusses the different techniques that have been used to achieve reconfigurable microwave filters. The reconfigurability is based on:

- Bank of Filters
- PIN diodes
- RF MEMS
- Optical Switching
- Varactors

3.1 BANK OF FILTERS

The concept of bank of filters evolved as a way to adapt the filter to different frequency bands [7]. It consists of switchable fixed frequency filters to support multiple frequency bands as shown in figure 3.1; the disadvantage of this technique is that it increases costs as well as size. New developments are focused on making more compressed and cost efficient reconfigurable filters that are based on electrical switching.

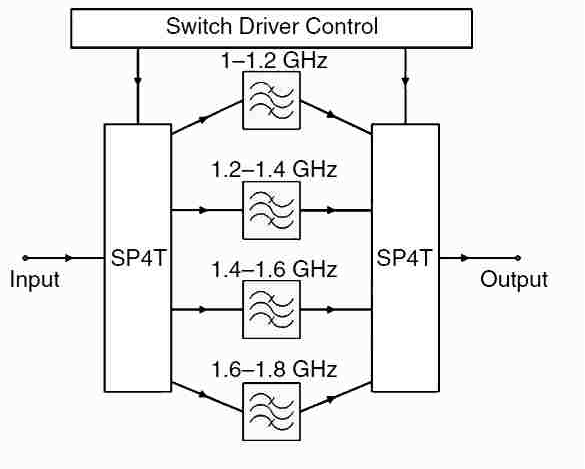

Figure 3.1: Example Bank of Filters [7]

3.2. PIN DIODES

PIN diodes switches have been used to achieve tunability in microwave filters. Their low cost implementation makes them very attractive components. For example, in [8] a two pole bandstop filter that implements PIN diode switches is presented. Figure 3.2 shows a diagram of the filter: four PIN diodes, D1, D2, D3, and D4 are located within the two $\lambda_g/2$ resonators. When all the PIN diodes are reverse biased the filter reaches a center frequency of 2GHz; conversely, when they are forward biased, the filter center frequency is 1.5 GHz.

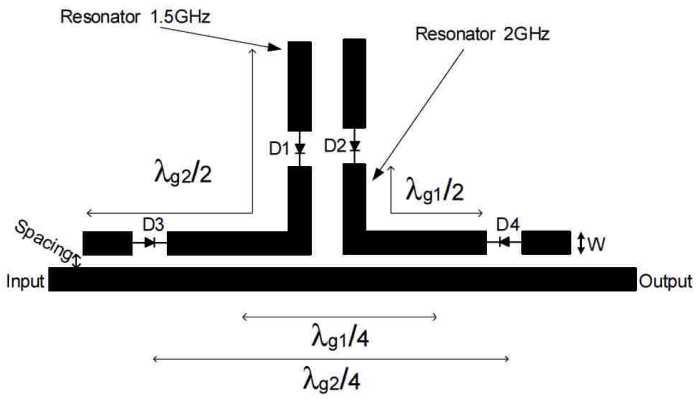

Figure 3.2: Diagram of the Bandstop Tunable Filter with Pin Diodes[8]

Moreover, a compact design of a UWB filter is reported in [9]. The reconfigurable filter uses PIN diodes to change its response from bandpass to bandstop. The filter, as shown in figure 3.3, consists of two cascade unit cells that are connected with an inductive stub. Each unit cell has two bended open stubs of size $\lambda_g/_4$, and a bended $\lambda_g/_2$ that connects the stubs. When the PIN diodes are activated, the filter behaves as a bandpass filter; and when they are deactivated, the filter behaves as a bandstop filter.

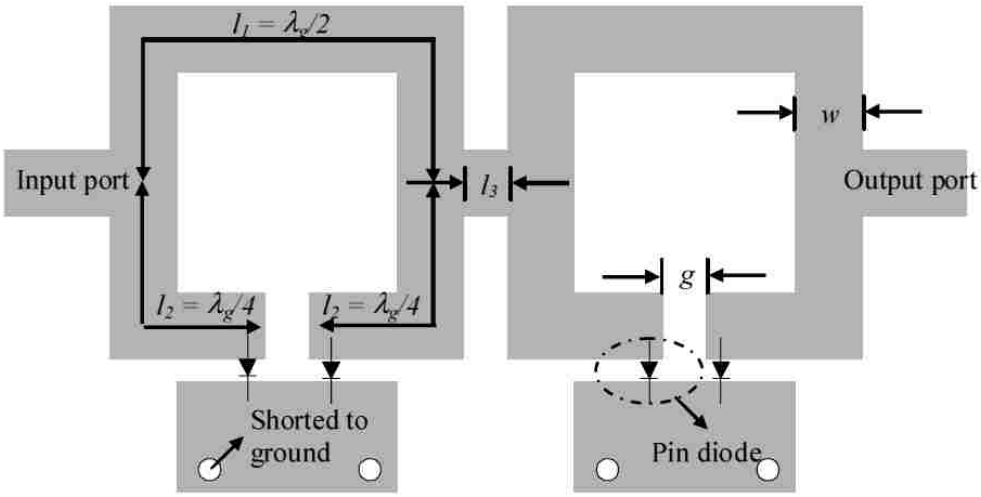

Figure 3.3: Bandpass to Bandstop Filter That Uses Pin Diodes as Switches[9]

3.3. RF MEMS

RF MEMS switches are also used to implement reconfigurable microwave filters. With this kind of switches, low cost and high linearity can be achieved. A MEMS switch consists of two metal plates; a fixed base plate and a variable film thin membrane. When the DC is applied, the movable membrane is attracted towards a metalized bottom contact (~0.3 μm aluminum) located on the substrate surface with an air hole in the silicon wafer. Figure 3.4 shows that when the applied voltage exceeds the pull down voltage of the switch the membrane falls over the bottom metal plate.

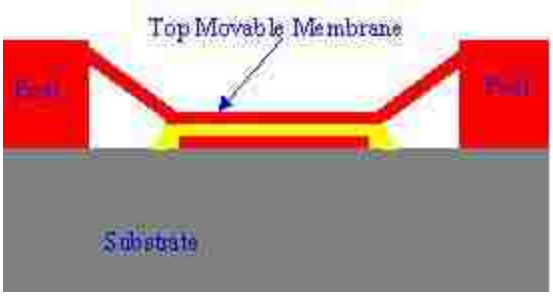

Figure 3.4: MEMs Switch

In [10] RF MEMS are used to obtain a tunable filter. The design consists of three pole resonators loaded by four pairs of switched MEMS capacitors. Each one of the switched capacitors is a series combination of a MEMs switch, and a fixed metal air metal (MAM) capacitor. The filter has 16 different combinations; (4-bit by 4 pairs of switched MEMs capacitors) each one of these combinations is able to change the effective electrical length of the resonators. The 16 responses cover the frequency band from 12.2 GHz to 17.8 GHz. The circuit model for this filter is shown in figure 3.5.

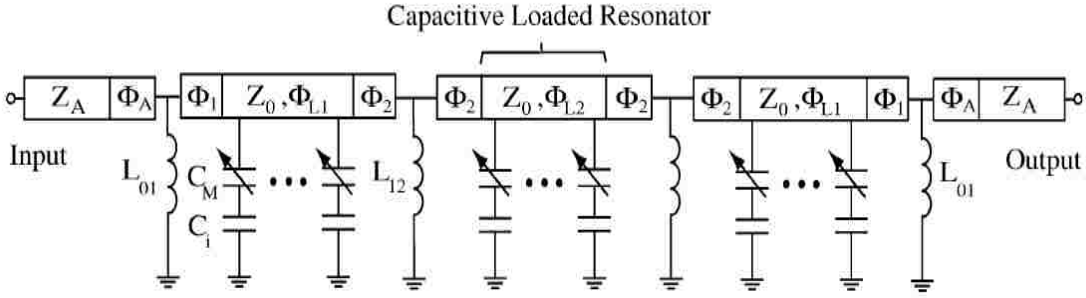

Figure 3.5: Circuit Model of a Three Pole Reconfigurable Filter Using Rf- MEMs[10]

A bandpass filter implements RF MEMs in [11]. This design also uses combinations of MEMs in series with MAM capacitors; these combinations create a 4-bit bank switched capacitors which is linked to a distributed shorted stub. The

variation of the capacitance is controlled by choosing the adequate value for the MAM capacitor. The schematic for this filter is shown in figure 3.6. The tuning range of this filter is from 8 to 16 GHz.

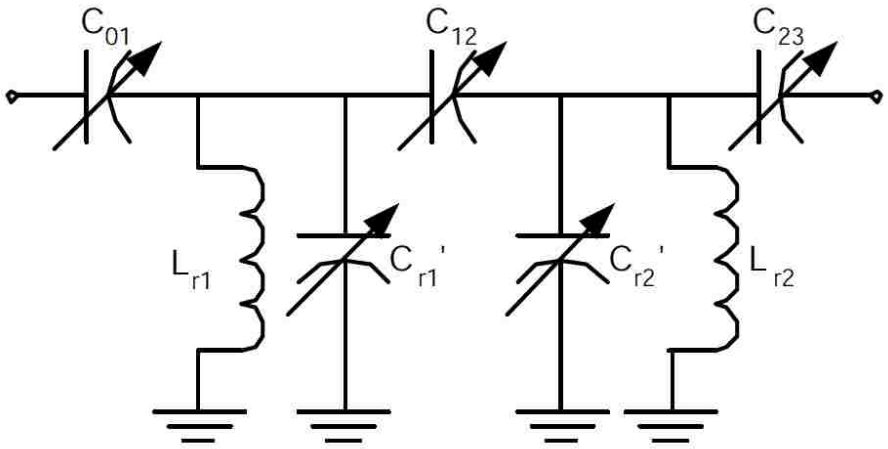

Figure 3.6: Schematic Bandpass Filter Using Rf MEMs[11]

3.6. OPTICAL SWITCHING

Optical switches are activated with light which is transmitted from a trigger light source. Optically controlled silicon switches have many advantages [12]: Immunity to electromagnetic interferences, low distorssion and cost-effectiveness. Tunability based on optical switches has been used in microwave filters. The filter shown in figure 3.7 behaves as a bandpass filter in the band between 3.1 GHz to 5 GHz.

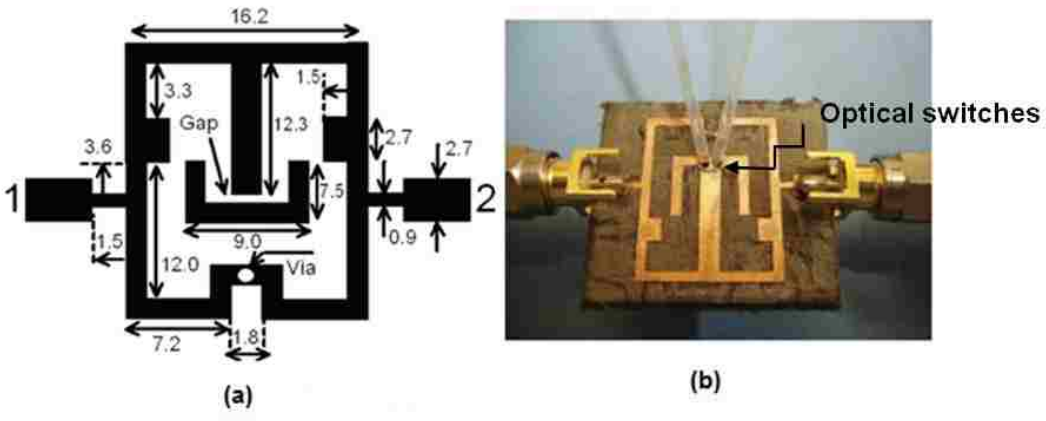

Figure 3.7: Structure Of The Filter, Layout (a) And Fabricated Prototype (b)[12]

The filter is a third order bandpass filter that has a $\lambda g/2$ resonator placed among a pair of $\lambda g/4$ short circuited resonators. The filter layout consists of lines with a width of 1.2 mm and a stub that is open circuited directing to a gap with a width of 2.4 mm. The structure of the filter, as shown in figure 3.7, has two short circuited resonator that are folded inwards, which allows the use of a common ground via. The open-circuited stub (located in the symmetry plane of the filter) creates a transmission zero at 4GHz when the length of the stub is $\lambda g/4$ (switch is off); on the other hand, when the switch is turned on, the length of the stub increases and the zero is generated at 2.2 GHz.

3.5. VARACTORS

A varactor consists of a PN junction diode that changes its capacitance based on the variation of applied bias voltaget. Barium Strontium Titanate (BST) varactors have been used in combline filters to achieve reconfigurability. In [13] a

combline filter is reported where all strips are grounded at the same end, which creates capacitive loading, thus generating a very practical filter.

In figure 3.8 a three-pole tunable combline filter is illustrated. In this filter, each microstrip line resonator length is shorter than a quarter wave length at the frequency of operation. The structure is loaded with a varactor at one end, and is short circuited at the other end; the shunt lines behave as inductive elements and resonate with the capacitors at a frequency that is bellow their quarter wavelength frequency. Here the biasing of the varactors is made by implementing a blocking capacitor in series with each varactor.

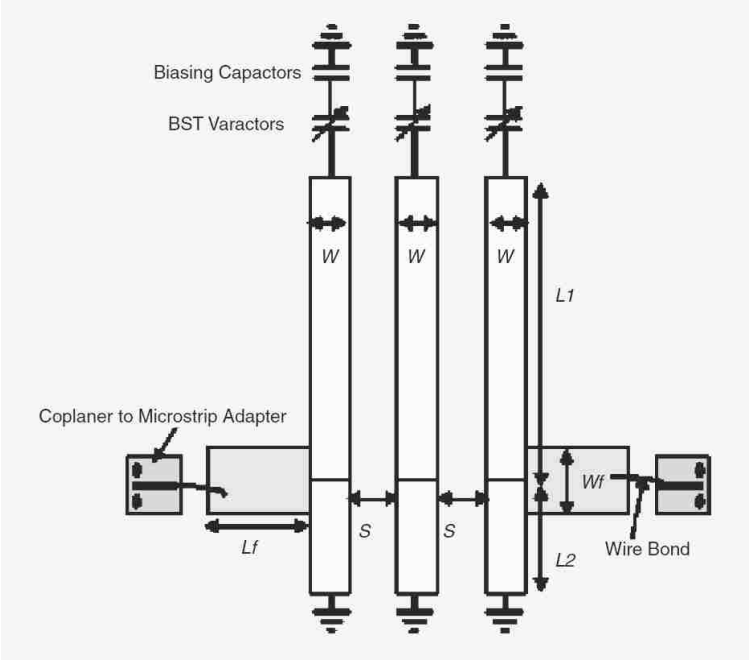

Figure 3.8: Reconfigurable Combline Filter Using Varactors[7]

Another design that uses varactors is reported in [14]. The bandpass patch filter consists of a triple mode circular patch resonator altered by four slots, each of these slots is able to perturb one or more of the fundamental degenerate modes ($TM^{z}_{1,1,0}$ - I, $TM^{z}_{1,1,0}$-II), and the second mode ($TM^{z}_{2,1,0}$). In fact, each slot can increase the current path; therefore it is able to reduce the resonant frequency of the filter. Varactors are implemented in this filter in order to alter the four slots, thus lowering the central frequency and the filter bandwidth. Two varactors are implemented per slot. Figure 3.10 shows a scheme of the filter with the implementation of the varactors.

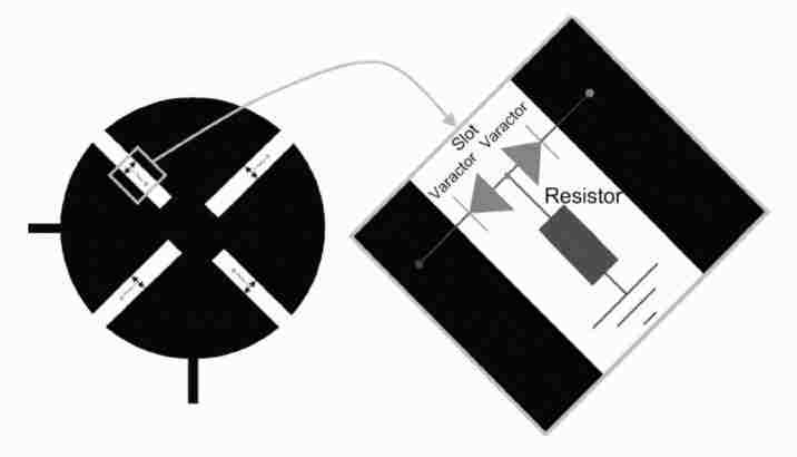

Figure 3.9: Bandpass Patch Filter with Varactors [14]

CHAPTER FOUR

RECONFIGURABLE BAND PASS AND BAND STOP FILTER INTEGRATED IN AN ANTENNA STRUCTURE FOR CR SYSTEM

New challenges in reconfigurable antenna design are arising as a result of recent developments in software–defined radio (SDR) and dynamic spectrum allocation. Antennas that are reconfigurable are becoming the centre of attention due to their ability to tune their operating frequency and keep the same radiation and gain characteristics.

One of the biggest challenges in reconfigurable antenna design for real applications is to maintain a constant gain at different resonant modes of the structure. One possible solution to this problem is to integrate a reconfigurable filter with the antenna structure. This technique will not alter the antenna surface current distribution and hence the radiation pattern will be less affected by the frequency tuning of the filter.

Two filtenna designs are shown in this chapter. The first design is a bandpass reconfigurable filter embedded into a Vivaldi antenna structure. The filter permits transmission at certain frequencies in the bandwidth of the antenna. The second design is a bandstop reconfigurable filter that is also embedded in a UWB antenna. Bsically the filter rejects the transmission at different frequencies. Both designs use copper tape stripes as switches as a proof of concept.

4.1 Integrated Cognitive Radio Antenna Using Reconfigurable Band Pass Filters for Interweave Cognitive Radio

In this section, a technique is proposed to achieve frequency reconfigurable antenna for a cognitive radio environment. This is accomplished by integrating a reconfigurable filter within the antenna structure. The tuning of the filter is based on the incorporated switches within the filter structure, as illustrated below in figure 4.1.

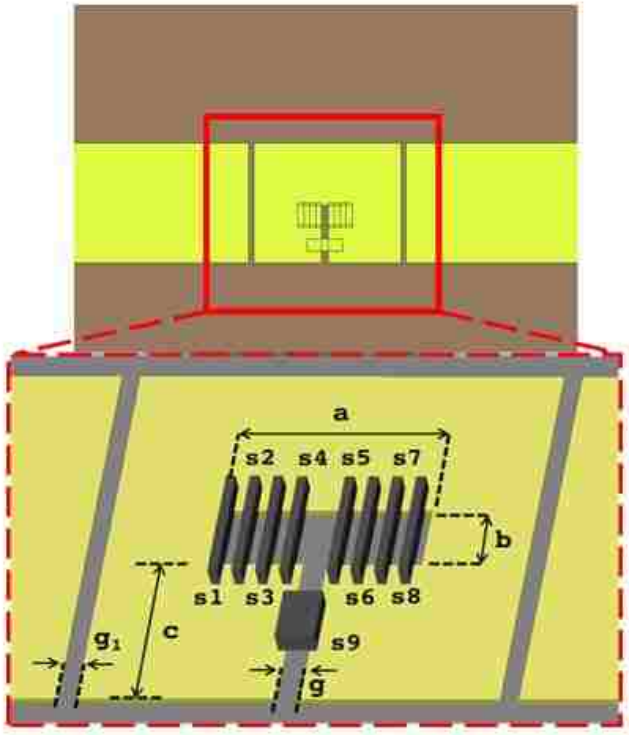

Figure 4.1: DMS Bandpass Filter. The switches are represented for s1-s9

The reconfigurable filter is a band pass filter that consists of a Defected microstrip structure (DMS); such structure adds slots within the microstrip generating resonant characteristics in the frequency response. The DMS has a T-shaped slot, of dimension 2.25 mm x 2.8 mm, and two coupling gaps at the

sides of the slot of dimension 0.25 mm each. The purpose of the gaps is to allow the filter to have the “band-pass” feature by functioning as a parallel-series resonance. The proposed design is printed on the Taconic TLY substrate with a dielectric constant ε_r=2.2 and a thickness of 1.6 mm. The filter reconfigurability is achieved by integrating 9 switches within the T-slot, which are activated in pairs of two from the two edges of the T-shape. The purpose of the switches is to change the length of the slot (labeled ‘a’ in figure 4.1) in order to produce a reconfigurable band pass filter. The different combinations of the switches are summarized below in table 1.

Table 1: Combinations of the Switches

Mode	Switches ON
0	*None*
1	*{s1, s8}*
2	*{s1, s8}, {s2, s7}*
3	*{s1, s8}, {s2, s7}, {s3, s6}*
4	*{s1, s8}, {s2, s7}, {s3, s6}, {s4, s5}*

4.1.1 EQUIVALENT CIRCUIT

The DMS structure can be expressed in terms of lumped elements by using circuit theory. The design is simulated with High Frequency Structure Simulator Software (HFSS). In order to extract each of the different resonant frequencies, the S-parameters matrix obtained is then exported to the Advanced

Design System (ADS). According with [19] the corresponding values for the capacitances and the inductances can be obtained from the next two equations.

$$C_{s,p} = \frac{f_c}{200\pi\left(f_0^2 - f_c^2\right)},\ L_{s,p} = \frac{1}{4\pi^2 f_0^2 C_{s,p}}$$

Where f_o is the resonant frequency and f_c is the cut-off frequency of the designed filter.

The change in the filter operating frequency will change the values of C and L as summarized in table 2.

Table 2: Values of C and L

Cs [pF]	Ls [nH]	Cp [pF]	Lp [nH]	Frequency [GHz]
0.778	*61.10*	*0.09913*	*1.142*	*9.4*
0.1772	*98.37*	*0.1064*	*1.064*	*9.78*
0.1675	*1.254*	*0.113*	*0.999*	*10.23*
0.1592	*1.188*	*0.1286*	*0.880*	*10.61*
0.1516	*1.239*	*0.147*	*0.7691*	*11.18*
0.1326	*1.288*	*0.2393*	*4.729*	*12.3077*

Figure 4.2 shows the equivalent circuit model for the DMS reconfigurable filter. The two gaps are modeled as parallel series LC and are represented by the inductor Ls and the capacitor Cs; as well as, the T-slot is modeled by Lp and Cp.

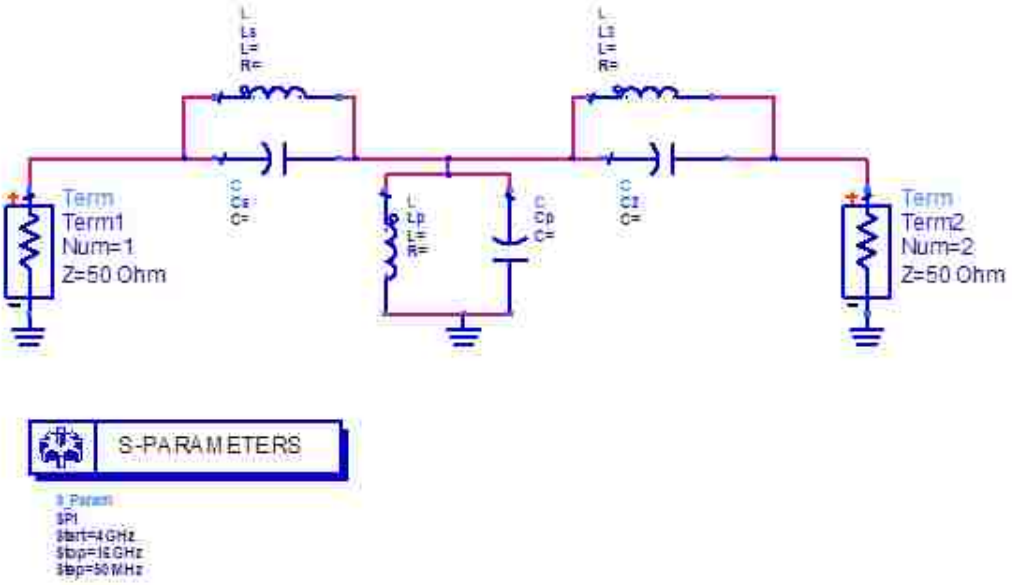

Figure 4.2: Bandpasss DMS Filter Equivalent Circuit

4.1.2 FILTER SIMULATIONS

The simulated results of the filter are shown in figure 4.3; for the 5 modes. It is important to notice that the behavior of the filter allows to pass certain frequencies between 9.4 GHz and 11.18 GHz band. The five modes of the filter are summarized in table 3.

TABLE 3: BANDPASS FILTER MODES

Mode	Frequency [GHz]
0	9.4
1	9.78
2	10.23
3	10.61
4	11.18

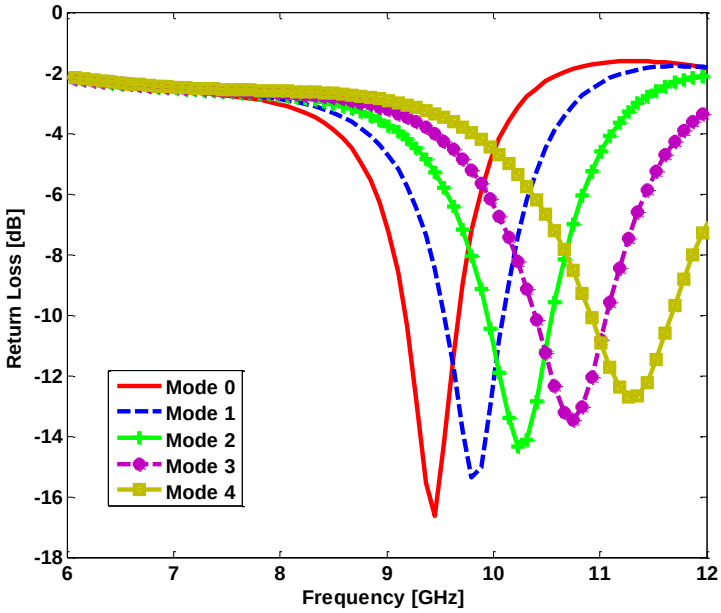

Figure 4.3: Simulated Filter Return Loss

4.1.3 Complete Design

The complete reconfigurable design involves a dual-sided tapered slot antenna (TSA). This antenna, also called Vivaldi antenna, has inner and outer contours that are curved based on an exponential function.

4.1.3.1. Vivaldi Antenna

The name of the Vivaldi antenna is due to the shape similarities to a cello or violin, instruments used by Antonio Vivaldi, a composer from the Baroque period, and who was the favorite composer of the antenna designer.

A Vivaldi antenna is a special TSA with planar structure which is easy to integrate with transmitting and receiving elements to form a solid structure. This antenna is classified in the category of continuously scaled, gradually curved, slow leaky end-fire travelling wave antennas. The TSA “has theoretically unlimited instantaneous frequency bandwidth” [33]. This frequency bandwidth extends from values bellow 2GHz to values above 40 GHz. A typical configuration of a Vivaldi antenna is shown in figure 4.4. The antenna consists of a metallic ground plane, a dielectric substrate, and a feeding microstrip transmission line.

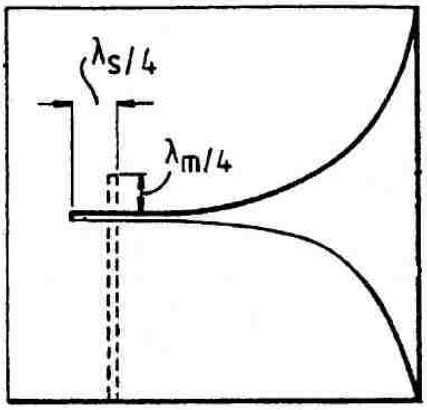

Figure 4.4: Typical Structure of a Vivaldi Antenna[33]

This kind of antenna is a surface travelling-wave antenna. Its propagation happens due to the phase velocity of its Electromagnetic (EM) waves, this phase velocity is less than the speed of light in free space. Therefore, the radiation pattern of the antenna has an end-fire radiation pattern as shown in figure 4.5.

The phase velocity and the guide wavelength depend of the thickness, and the dielectric constant of the substrate as well as the taper design.

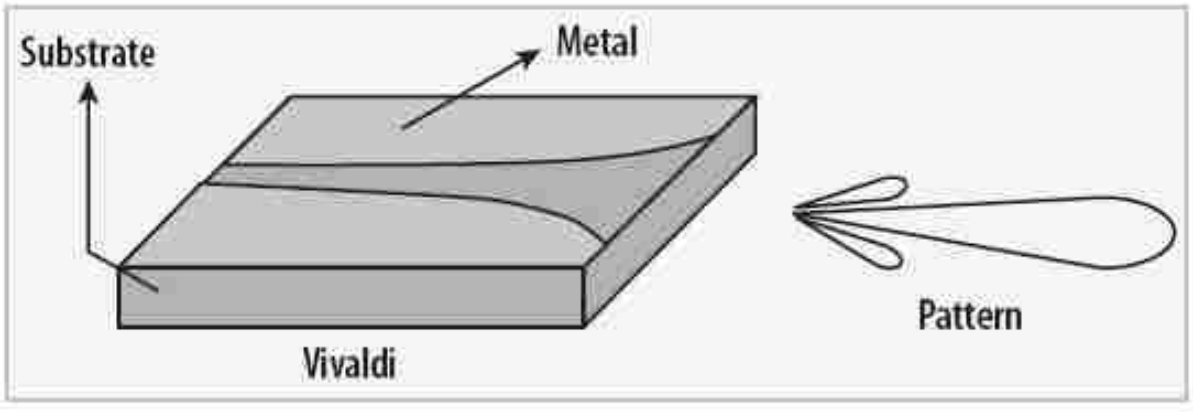

Figure 4.5: Vivaldi Antenna and Its Corresponding Radiation Pattern[17]

Different taper profiles can be used for a Vivaldi antenna. For designing the antenna, an exponential expansion function $y = \pm Ae^{PX}$ is used, where p is the magnification factor that establishes the beamwidth; 'y' defines the separation between the conductors and x represents the length. When x is positive and big, the energy will have abandoned the guiding structure and the curve truncates; likewise, when x is also big but negative the wave remains bound to the conductors and the generated radiation is small, and a truncation in the curve may occur as well.

The expression for the performance of a Vivaldi aerial fabricated on alumina substrate is given by:

$$y = \pm 0.125\, e^{(0.052x)}$$

The Vivaldi antennas are specially attractive because they generate a symmetrical end-fire beam with high gain and low side lobes; in addition, they can be designed for linearly polarized waves. Moreover, if they are fed with a shift of 90 degrees in phase for orthogonal devices they will be able to transmit and receive circularly polarized waves.

4.1.3.2. INTEGRATION WITH THE RECONFIGURABLE FILTER

The DMS filter is integrated on the microstrip feed line of the antenna structure. Such configuration allows the antenna to be reconfigurable based on the mode of operation of the filter. The complete design was simulated in HFSS, and the corresponding structure is shown in figure 4.6. In the top layer there is the feeding line, where the filter is located, with a length of 32.28mm. In the bottom layer of the design; there is the ground plane of the filter, within the partial ground plane for the antenna with total dimensions of 40mm x 32.28 mm. The total size of the design is 65mm x 40 mm

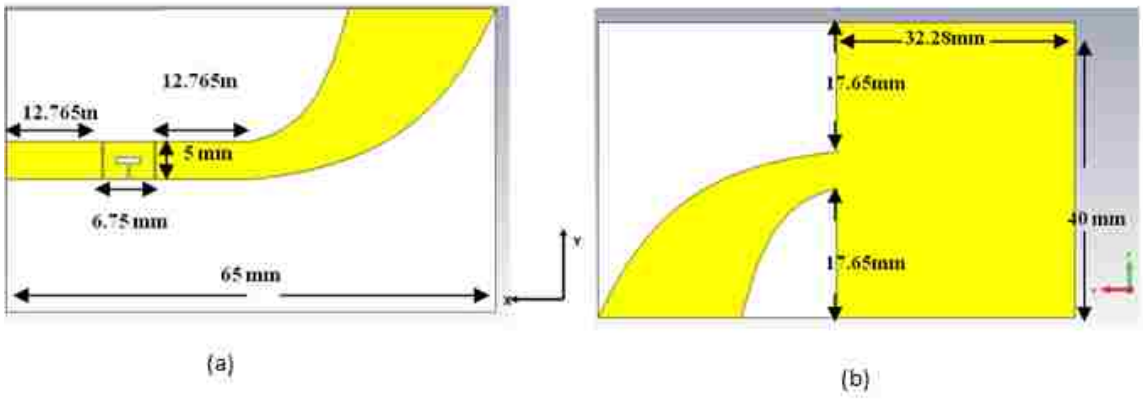

Figure 4.6: Dimensions of the Prototype Top and Bottom Layers

4.1.4. EXPERIMENTAL RESULTS

The filtenna is etched using the LPKF ProtoMat s62 machine onto the Taconic TLY substrate with ε_r=2.2 and thickness of 1.6 mm. The fabricated prototype is shown in figure 4.7. The top layer is located at the left side of the picture, while the right part of the picture is the bottom layer where the ground plane is shown.

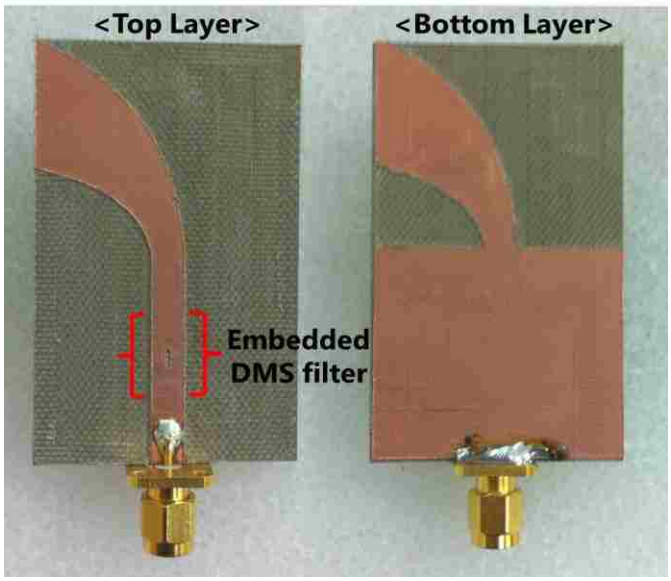

Figure 4.7: Fabricated Prototype

There are four cases for the reconfigurable filter integrated with the TSA antenna. One can notice how the antenna is able to tune its operating frequency by changing the status of the switches within the T-slot of the reconfigurable filter as shown in figure 4.8. The tuning frequencies of the integrated antenna are

shown in Table 4. It is important to mention that the antenna/filter combination of has the effect of lowering the band-pass frequency of the DMS filter.

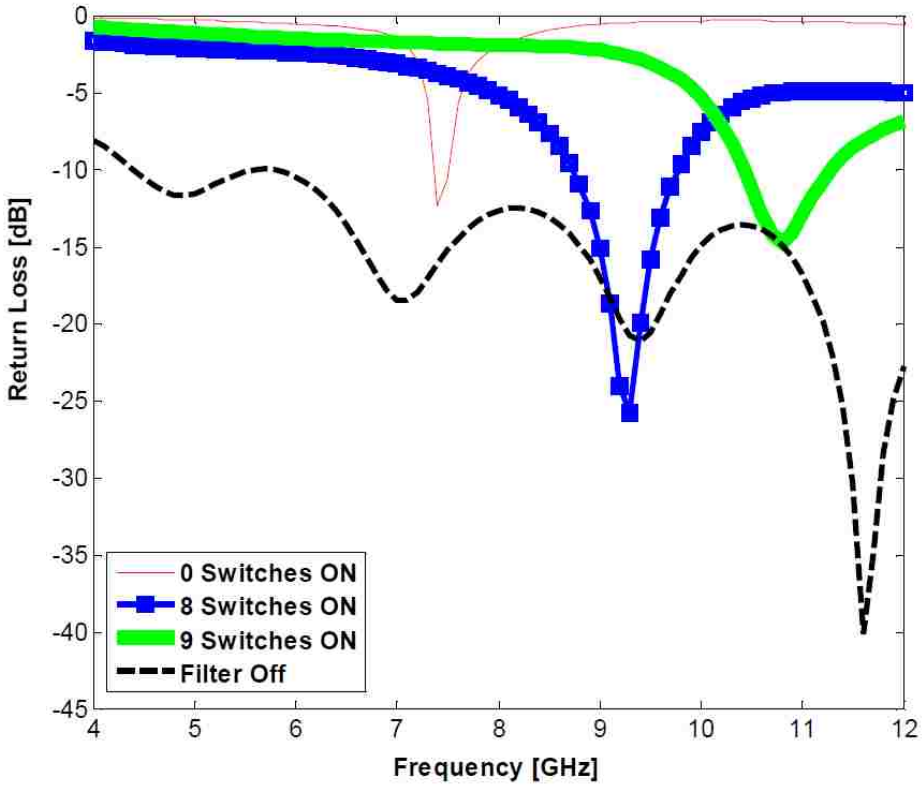

Figure 4.8: Four Cases for the T Slot Reconfigurable Filter

Table 4: Frequency Tuning for Each Mode

Switches ON	**Frequency**
0	7.4 GHz
{s1, s8}, {s2,s7}, {s3, s6}, {s4, s5}	9.3 GHz
All On	10.8 GHz
Filter Off	All Pass

The fabricated prototype was tested by using the HP 8510C Network Analyzer. In order to compare simulated data versus measured data, it is useful to see each one of the modes separately. The following two figures (4.9 and 4.10) show the comparison between the simulation and the measurement for the different modes of the filtenna. It can be noticed that a good agreement is obtained.

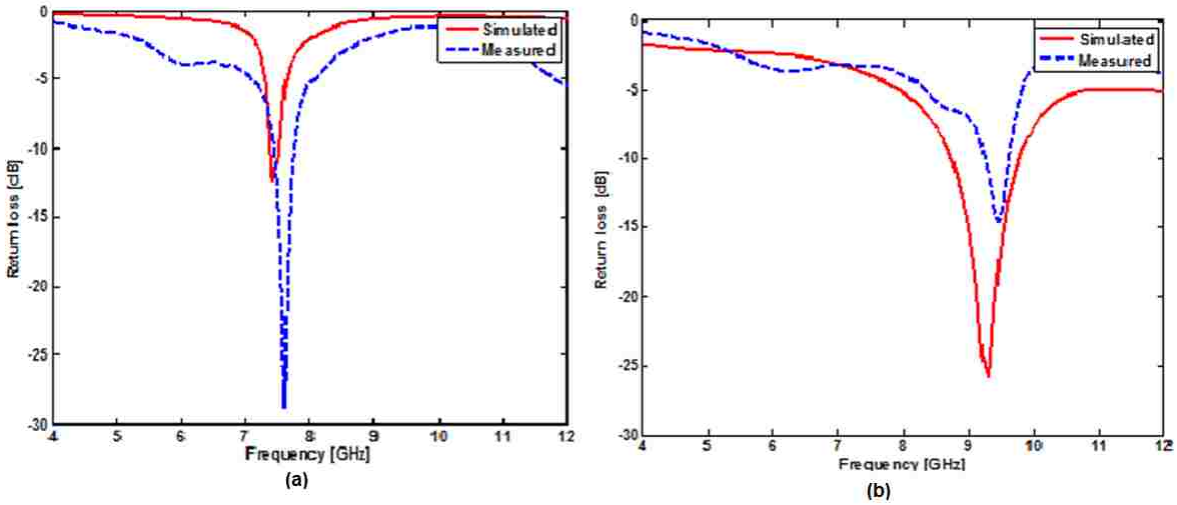

Figure 4.9 : Simulation Vs Measurement of the Prototype for (a) No Switches On. (b) Two Switches

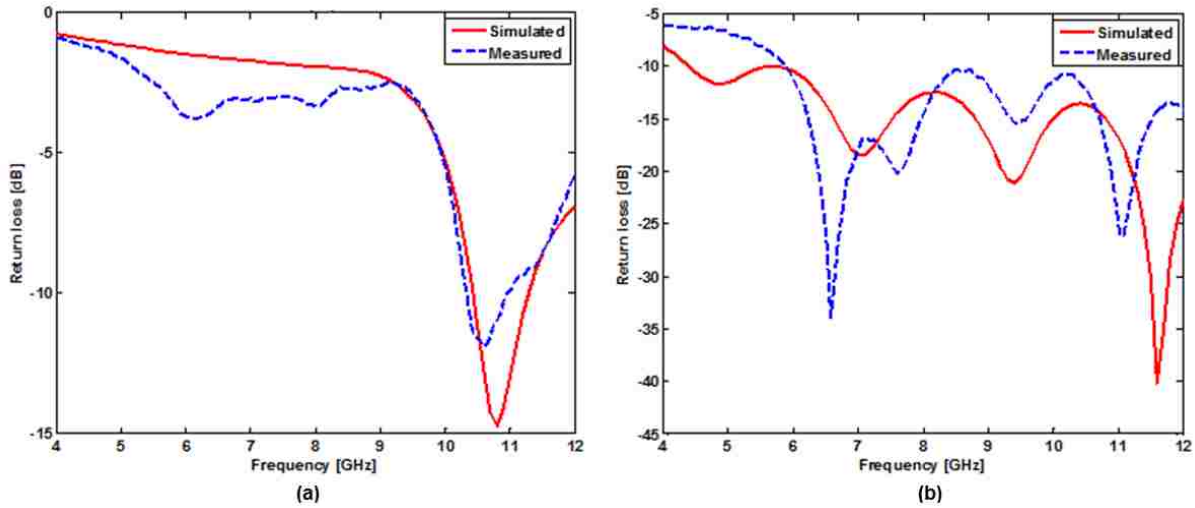

Figure 4.10: Simulation vs. Measurement of the Prototype for (a) All Switches on. (b) Filter Off

Also it is shown in figure 4.10 (b) that when the band pass filter is deactivated the antenna preserves its UWB response.

The normalized antenna radiation pattern for the different modes in the YZ plane is shown in figure 4.11. An almost Omni-directional radiation pattern is obtained.

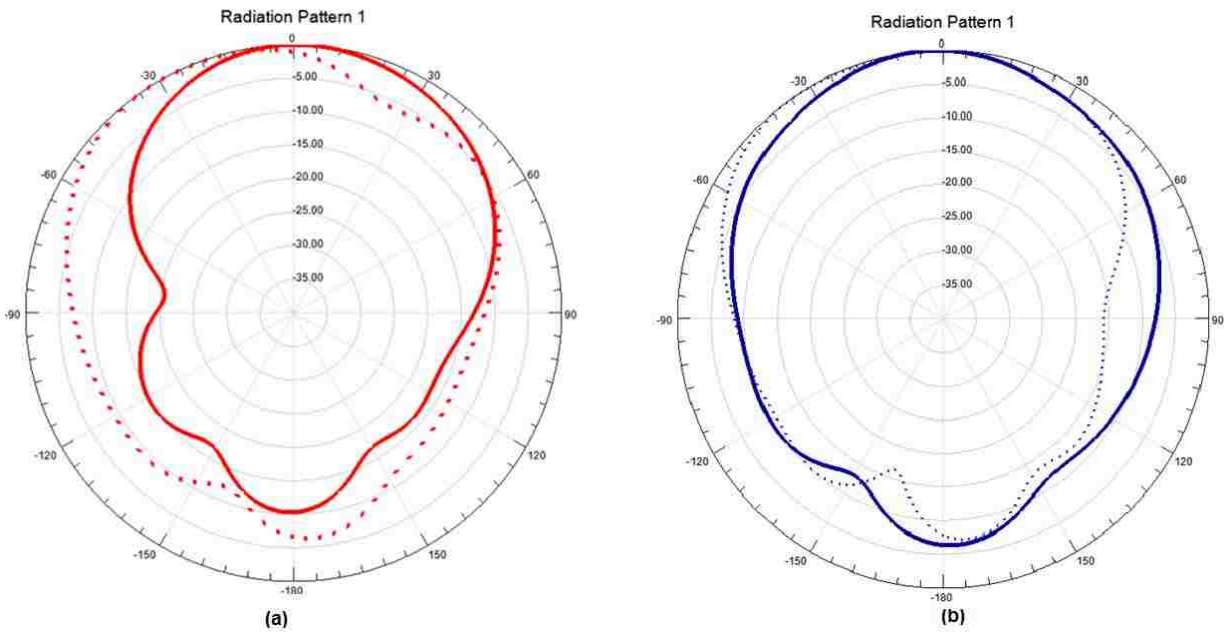

Figure 4.11: Normalized Radiation Pattern for (a) 0 Switches On(solid) and 8 Switches On (dotted). (b) 9 Switches On (solid) Filter Off (dotted)

Figure 4.11:

The importance of the proposed design in cognitive radio communication is that can be operated as a sensing antenna when the filter is off. After band scanning, the antenna can function as a communicating antenna by means of manipulating the switches on the DMS filter.

4.2 Reconfigurable Band Stop Filter Embedded Into An Antenna For UWB Underlay Cognitive Radio Environment

A new design of a reconfigurable band-stop filter based on a defected ground structure (DGS) is fabricated and presented in this section. The Defected Ground Structure consists of a U-shape slot located in the ground plane and parallel to the microstrip feeding line of the antenna.

4.2.1 Filter Design

A DGS is an etched-defect of the ground plane that alters the ground current distribution; this alteration can generate a change in the capacitance and in the inductance of a transmission line; and due to this alteration, these structures can produce a rejection band in adetermined frequency range. The combination of DGS with microstrip produces a resonant character in which frequency is controlled by altering the dimensions of the slot.

This DGS filter acts as a band reject filter in the frequency band between 2.5 GHz and 4 GHz. Figure 4.12 shows the filter design that is printed on the Taconic TLY substrate with a dielectric constant $\varepsilon_r = 2.2$ and a thickness of 1.6 mm. The filter becomes reconfigurable by integrating 3 switches: One single switch S1 that deactivates the filter and one pair of switches {S2, S3} located in the columns of the U slot. When the length of the U slot is altered a notch is generated at a frequency proportional to the slot length.

Table 5: Modes for the DGS Filter

Modes	Frequency
1	All Pass
2	3.08 GHz
3	2.5 GHz
4	4 GHz

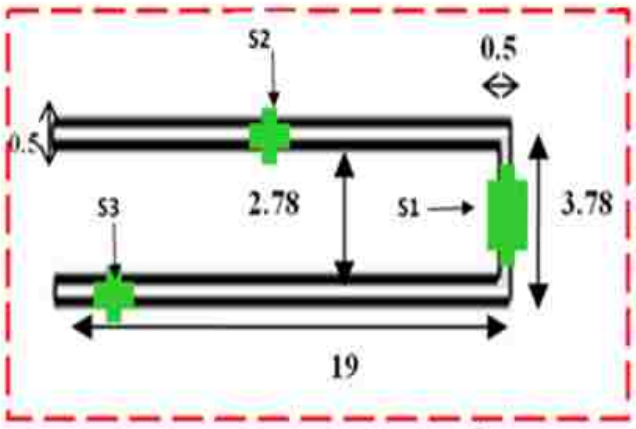

Figure 4.12: Structure of the DGS Bandstop Filter

Different switch states for the 4 modes of operation:

Mode 1:S1: ON

Mode 2: All OFF

Mode 3:S1: OFF S2: ON; S3:ON

Mode 4: S1: OFF; S2: OFF;S3:ON

4.2.2 Filter Simulations and Measured

The filter was simulated in HFSS, fabricated also by using the ProtoMat s62 machine and tested with the HP 8510C Network Analyzer. The responses for the simulated and measured results are shown in figures 4.13 and 4.14 respectively. This design reflects an efficient rejection at the band frequency since the notches reach 0dB which means no transmission.

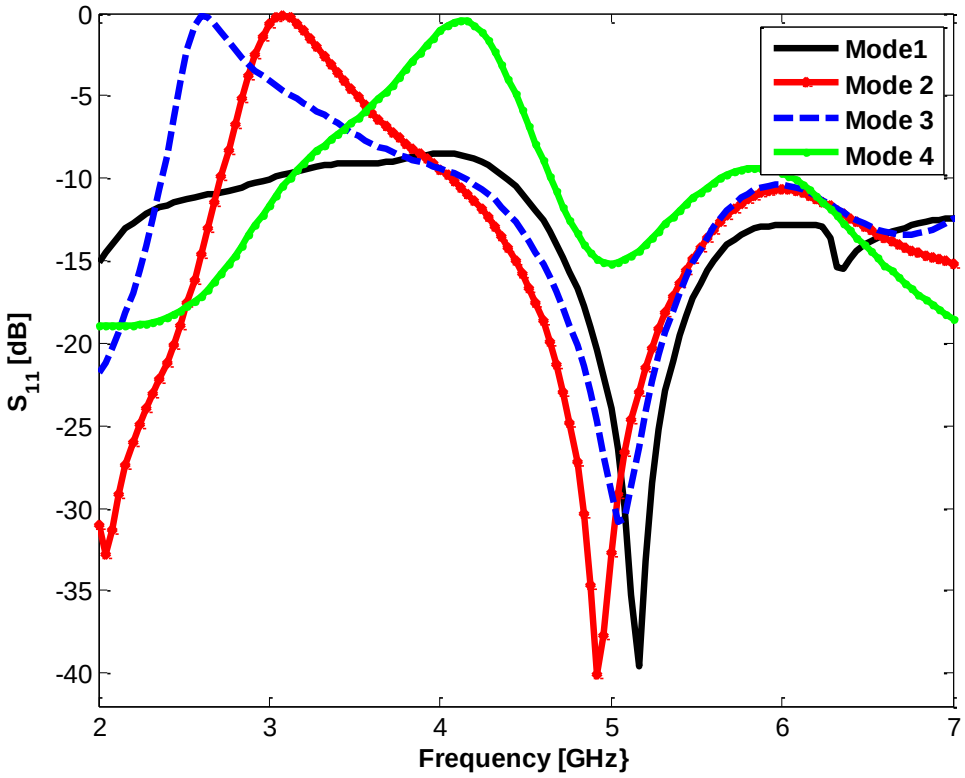

Figure 4.13: Simulation Results for the Different Modes of the Filter

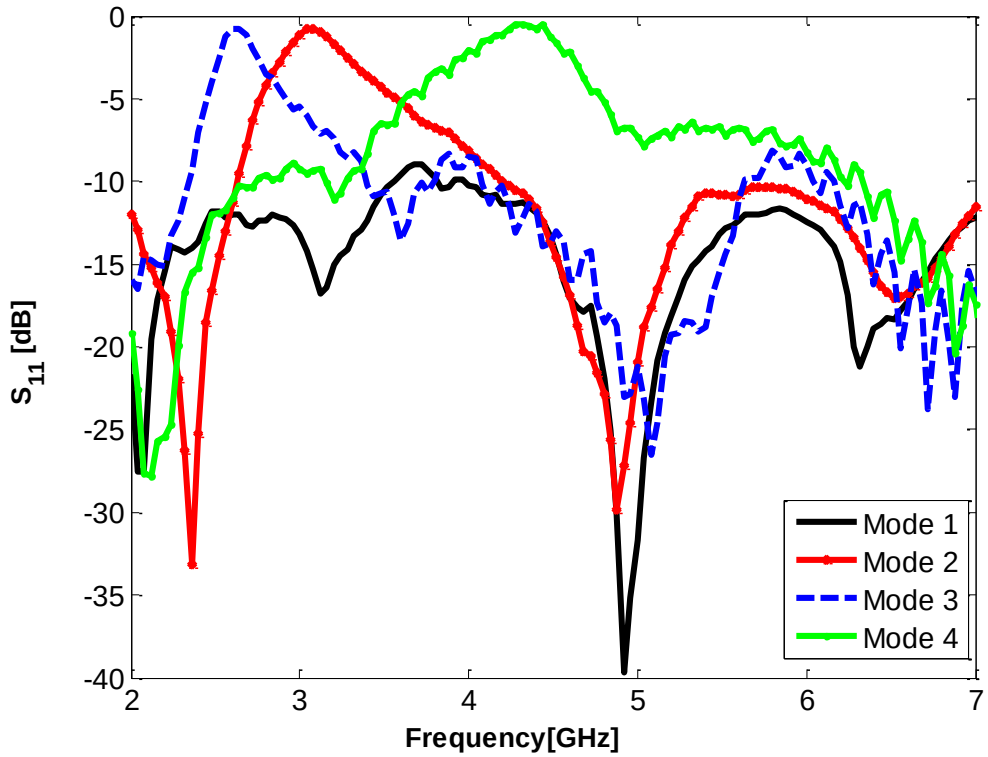

Figure 4.14: Measured Results for the Filter

4.2.3. COMPLETE DESIGN

The complete design with the integrated antenna is shown in figure 4.15(a). The antenna selected for this design is an ultra-wide band antenna that operates in the frequency range of 2 GHz to 10 GHz.

Figure 4.15(b) shows the fabricated prototype. The structure is printed on the Taconic TLY substrate with a dielectric constant $\varepsilon_r = 2.2$ and a height of 1.6 mm. The dashed rectangle shows the position where the filter is located, parallel to the feeding line.

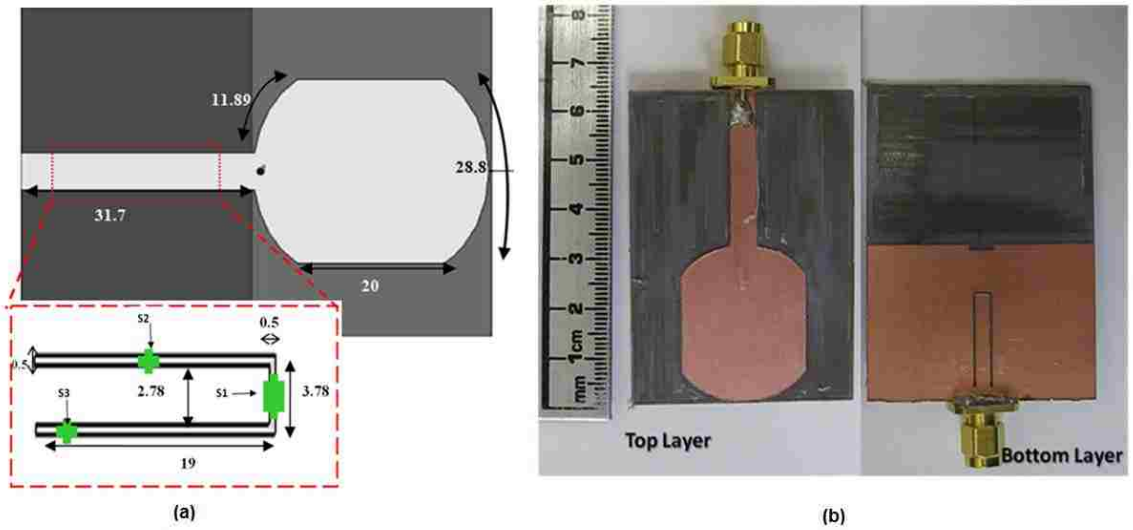

Figure 4.15: The UWB Antenna Structure

4.2.4. Simulation Vs Results for the Complete Design

The results for the simulation are compared with the measured data obtained from the fabricated prototype.

Figure 4.16 shows the comparison for modes 1 and 2, while figure 34 shows the comparison for modes 3 and 4. Good agreement is noticed between simulation and measurement in all four cases, and most importantly the plots reflect that the filtenna is able to reach 0 dB for the simulated as well as for the measured data, meaning that it perfectly blocks transmission for different frequency bands.

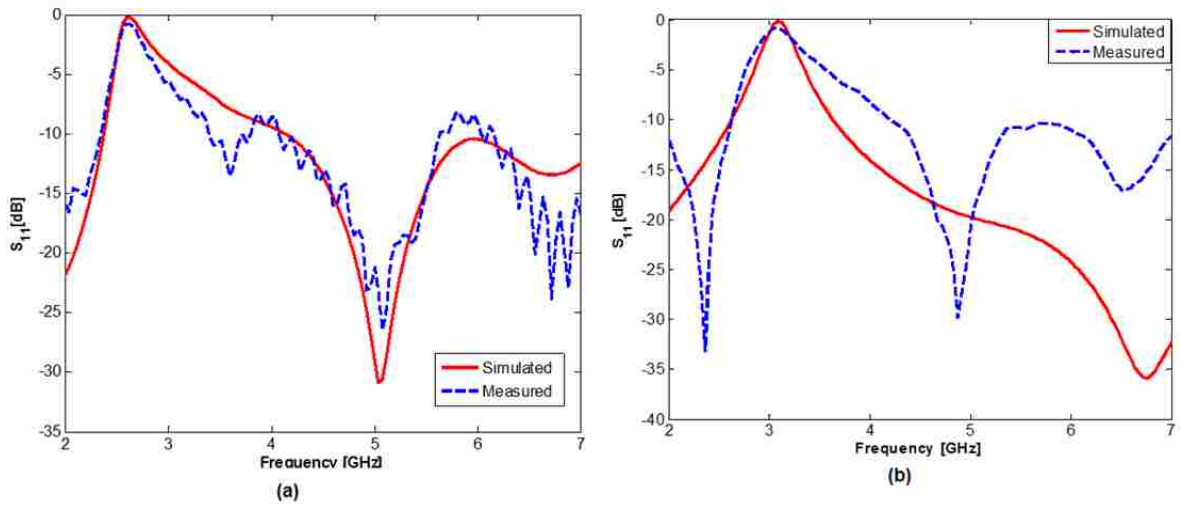

Figure 4.16: Simulated Vs Measured Data for Mode 3(A), And Mode 2(B)

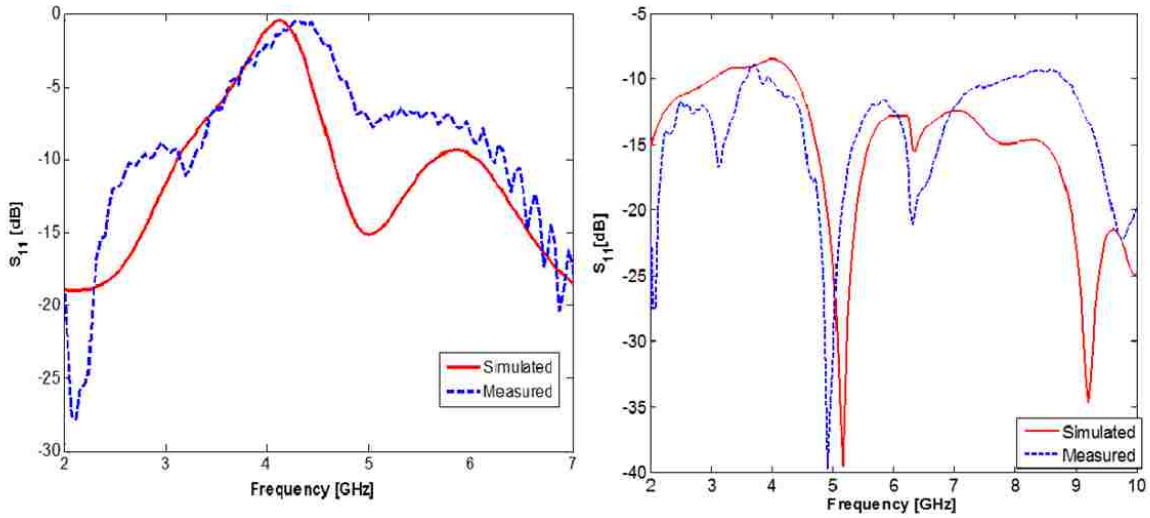

Figure 4.17: Simulated Vs Measured Data for Mode 1 (Left), And Mode 4 (Right)

The right side of figure 4.17 shows that when the filter is deactivated (Mode 1) the antenna has its UWB response; this occurs when S1 is turned on and the other two switches are turned off.

CHAPTER FIVE

A VARACTOR BASED RECONFIGURABLE FILTENNA

5.1. FILTER DESIGN

The final design uses a DMS band pass filter, printed on Taconic TLY, with a dielectric constant of $\varepsilon_r = 2.2$, of total dimensions of 30mm x 30 mm, and a height of 1.6mm. The filter, as shown in figure 35, is based on three microstrip lines at the top layer with a width of 5mm corresponding to 50Ω. Two side microstrips with length 9.6mm each, are connected to two input ports, and separated from the middle microstrip by gaps with fixed capacitances that allow the filter to have the bandpass behavior. The left gap size is 0.4 mm, while the right gap size is 0.6mm. The center microstrip is where the hexagonal DMS is located, and also where the varactor is placed. When different voltage values are applied to the varactor, the total structure capacitance changes and here is when the filter tunability takes part. The ground plane of the filter is the entire bottom part of the substrate.

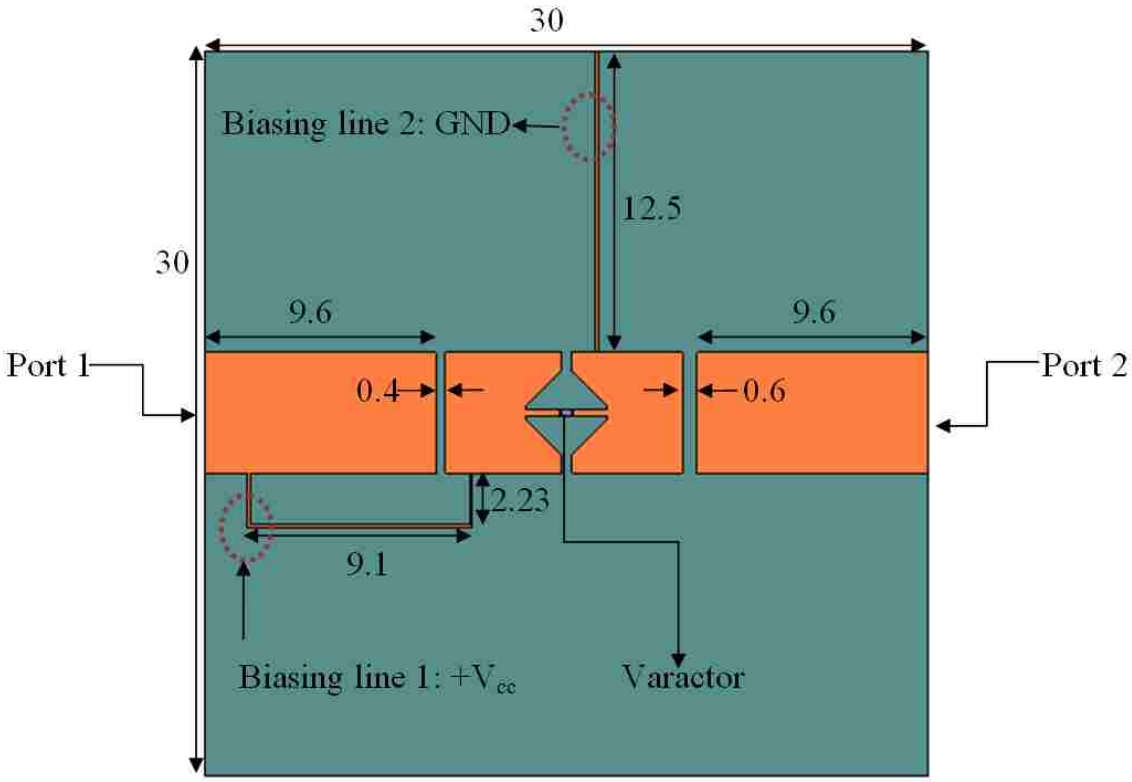

Figure 5.1: Dimensions of the Filter

5.1.1. VARACTOR BIASING

For the final filter design, the biasing of the varactor is done by adding a small bias line (biasing line 1) of width 0.1 mm that connects the middle microstrip, where the varactor is located, to the left microstrip, which is also connected to Port 1. This port is attached to a BiasT-DC Block (BT-V000-HS) which has the function of allowing RF signals and DC voltage in order to feed the filter. The varactor is grounded by using another bias line (biasing line 2), also with a width of 0.1 mm; this line connects the other end of the varactor to the ground plane which is the substrate bottom face.

A bias tee is used to feed the varactor in order to avoid external biasing lines that generate undesired signals in the resonance frequency of the filter. The bias tee is used to inject DC currents or voltages in RF circuits; it feeds the design without affecting the RF signal through the main transmission path. The schematic of the bias tee (figure 5.2) shows the capacitor that prevents DC signals to go back to the voltage source, and an inductor which protects the RF signals of the circuit. Figure 5.3 shows the physical structure of the bias tee.

Figure 5.2: Bias Tee Schematic

Figure 5.3: Bias Tee Model Bt-V000-Hs from UMCC

5.2 Filter Simulation and Measurement

The filter design that behaves as a bandpass filter is simulated using HFSS. The varactor is simulated with a rectangle shape sheet for which are

given the attributes of a capacitor lumped element. The circuit is complete by bridging the hexagon with the varactor. The prototype is printed with the LPKF ProtoMat S62 machine onto the already mentioned Taconic TLY substrate material. The fabricated bandpass filter is shown in figure 38.

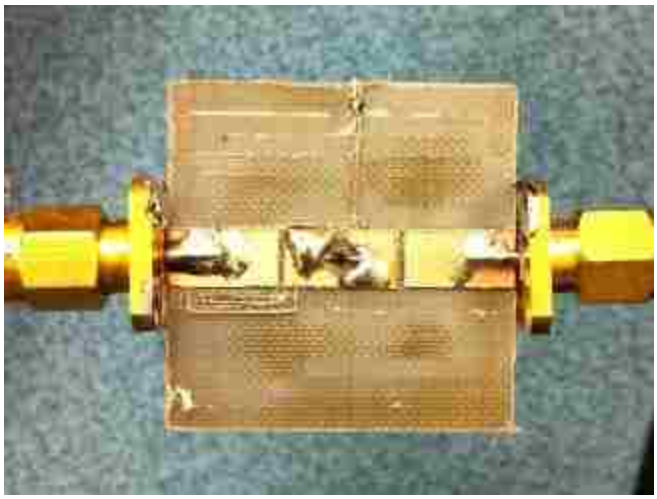

Figure 5.4: Fabricated Prototype for the Filter

The fabricated prototype is tested by using the HP 8720D Network Analyzer. The next two figures show the return loss simulations and measurements for different capacitance values of the varactor. According with the plots, there is a good agreement between the simulated and the measured data. Therefore, the filter behaves as a reconfigurable band pass.

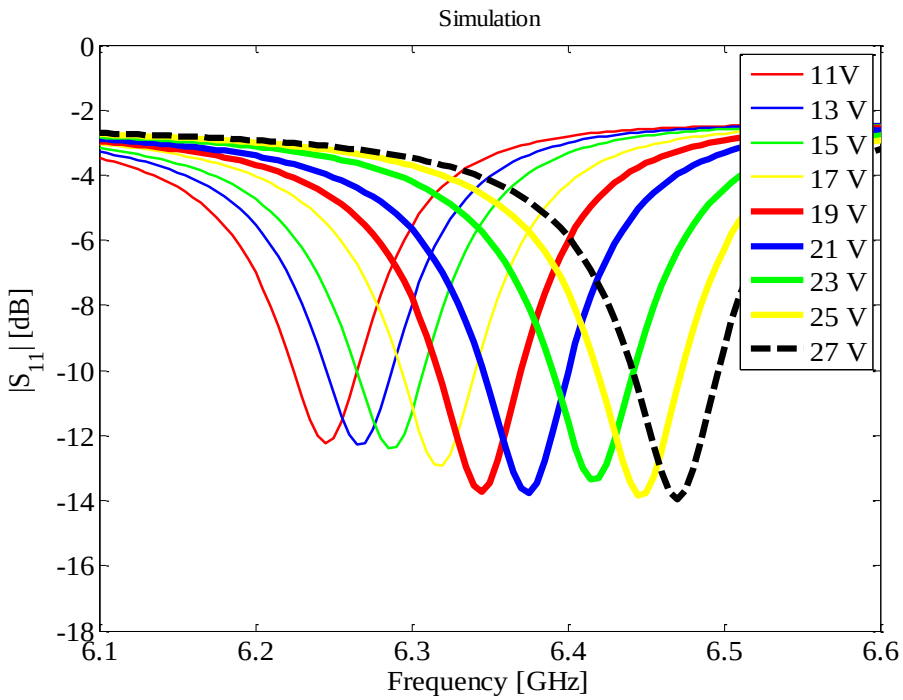

Figure 5.5: Filter Simulation

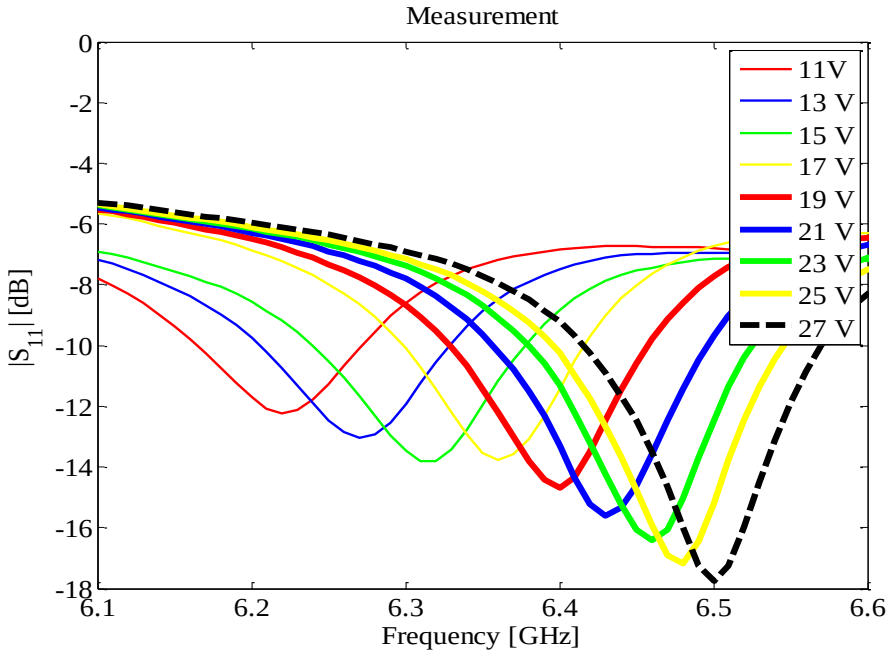

Figure 5.6: Mesured Data for the Filter

5.3 Complete Design of the Filtenna

A Vivaldi antenna is also chosen for the final design. The integration with the filter is accomplished by integrating the filter at the feeding of the antenna. The overall dimensions of the filter structure remain the same which means that the ground plane for the filtenna is 30mm x 30mm. The whole structure dimension is 59.8mm x 30mm. The fabricated prototype is shown in the figure 5.7:

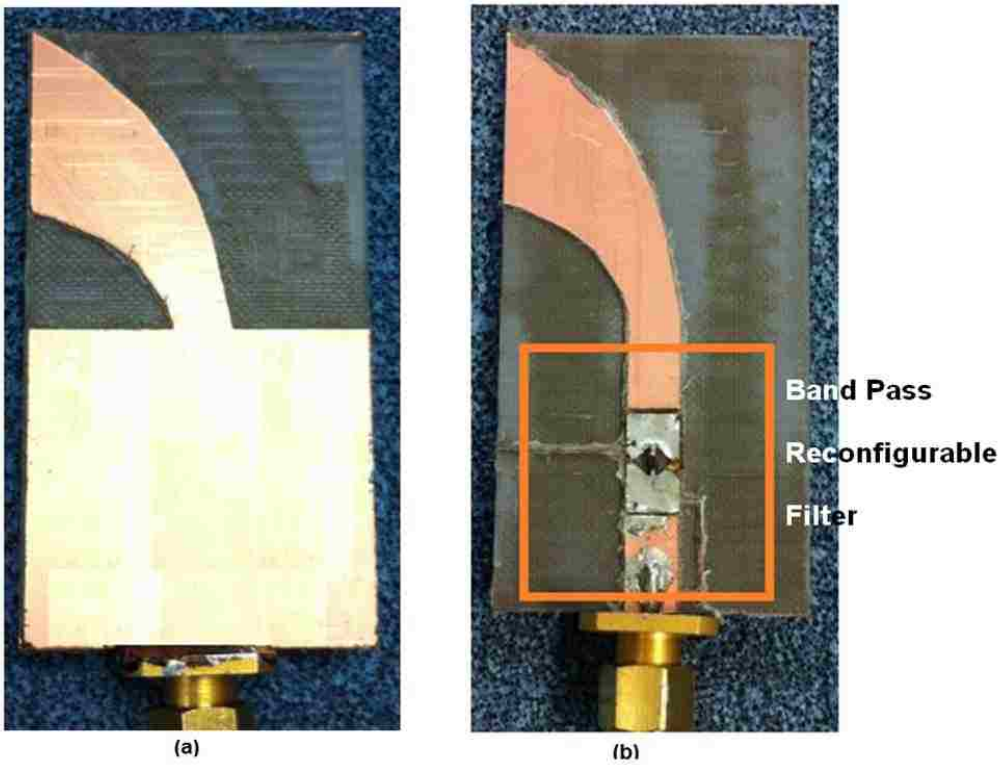

Figure 5.7: Fabricated Prototype (a) bottom layer, (b) top layer

The next two figures show the simulated results for this filtenna (figure 5.8) and measured results (figure 5.9). One can notice that the antenna can tune its frequency of operation depending on the modes of the filter.

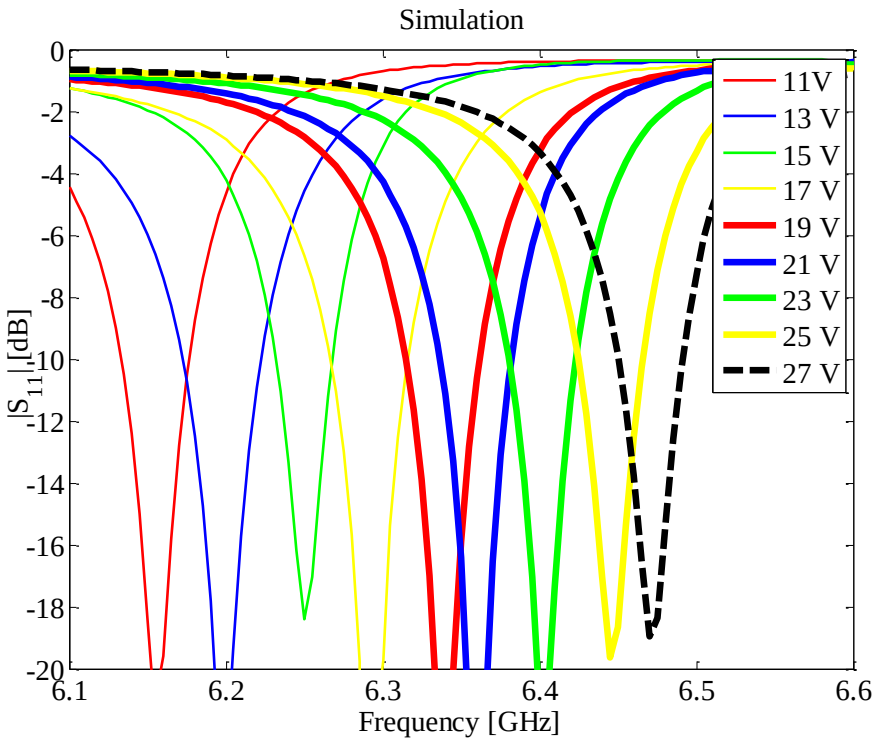

Figure 5.8: Simulated Results for th//e Complete Design

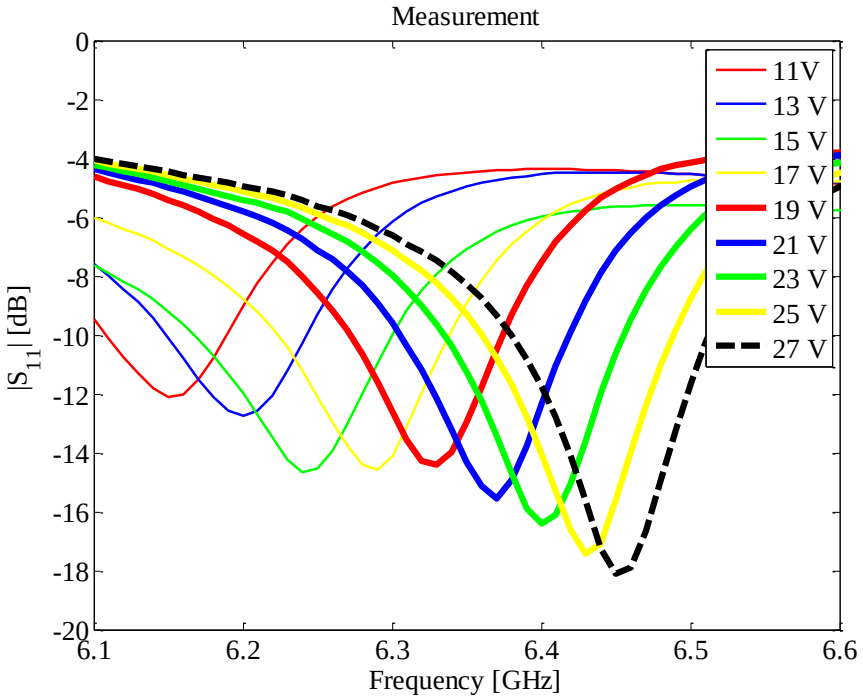

Figure 5.9: Measured Results

CHAPTER SIX

CONCLUSIONS & FUTURE WORK

In this work, we demonstrated that a filtenna can be implemented for a cognitive radio system. The reconfigurability is achieved by tuning the operation of a filter that is integrated within the antenna feeding line. A reconfigurable band-pass and band-stop filter were designed and tested. Good agreement was achieved between the simulated and measured data. Finally, a varactor based band-pass reconfigurable filtenna for interweave cognitive radio system was designed, fabricated and tested.

For future work we are looking to implement a reconfigurable band reject filter using active components (PIN diodes or Varactors). The same integration technique with the antenna structure will be adopted. Also we are looking to study reconfigurable filters that switch between band pass or band stop operation in order to have one antenna structure for both interweave and underlay cognitive radio environment.

REFERENCES

[1] D. Pozar, “Microwave Engineering”, 2nd Edition, J. Wiley, 1998, EEE194 RF Microwave Engineering.

[2] Y. Tawk, M. Bkassiny, G. El-Howayek, S. Jayaweera, K. Avery, and C. G. Christodoulou, “Reconfigurable front-end antennas for cognitive radio applications,” vol 5, No 8,pp 985-992, June2011

[3] G. Vazques Vilar. “Interference Management in Cognitive Radio Networks” 2010-2011. http://www.gonzalo-vazquez-vilar.eu/cognitive-radio.htm.

[4] Y. Tawk, J. Costantine, K. Avery, and C. G. Christodoulou, “Implementation of a cognitive radio front-end using rotatable controlled reconfigurable antennas,” *IEEE Transactions on Antennas and Propagation,* vol.59, no.5, pp.1773- 1778, May 2011.

[5] Y. Tawk, S. K. Jayaweera, C. G. Christodoulou and J. Costantine, “A comparison between different cognitive radio antenna systems,” International Symposium on Intelligent Signal Processing and Communication Systems, Dec. 2011

[6] S. Srinivasa, S. A. Jafar, “The Throughput Potential of Cognitive Radio: A Theoretical Perspective” 07 May 2007.

[7] P.W. Wong, I. Hunter. “Electronically Tunable Filters”. IEEE Microwave magazine October 2009.

[8] Z. Brito-Brito, I.Llamas-Garro, L. Pradell-Cara, A. Corona-Chavez . “Microstrip Switchable Bandstop Filter using PIN Diodes with Precise Frequency and Bandwidth Control”. Proceedings of the 38th European Microwave Conference.

[9] M. F. Karim Yong-Xin Guo , L. C. Ong, “Miniaturized Reconfigurable Filter Using PIN Diode For UWB Applications”. IEEE 2008.

[10] K. Entesari, G.M. Rebeiz. “A 12–18-GHz Three-Pole RF MEMS Tunable Filter”. IEEE Transactions, Vol. 53, No. 8, August 2005.

[11] K. Yan Lee,G.M. Rebeiz. “A Miniature 8–16 GHz Packaged Tunable Frequency and Bandwidth RF MEMS Filter”. IEEE International Symposium on Radio-Frequency Integration Technology,2009.

[12] L. Athukorala, K. Rabbi, C. Panagamuwa, J.C. Vardaxoglou, M. Philippakis, D. Budimir “Optically reconfigurable Microstrip UWB Bandpass Filters” 2010 Loughborough Antennas & Propagation Conference .

[13] J. Nath, D. Ghosh, J.Maria, A.I. Kingon, W. Fathelbab, , P. Franzon, M. B. Steer. “An Electronically Tunable Microstrip Bandpass Filter Using Thin-Film Barium–Strontium–Titanate (BST) Varactors,” IEEE transactions on microwave theory and techniques, vol. 53, no. 9, September 2005.

[14] A. L. Serrano , T. P. Vuong, F. Correra , P. Ferrari. “A Tunable Bandpass Patch Filter with Varactors”. IEEE 2010.

[15] K. Entesari, G. M. Rebeiz, “A Differential 4-bit 6.5–10-GHz RF MEMS Tunable Filter” *IEEE* transactions on microwave theory and *techniques*, vol. 53, no. 3, march 2005.

[16] A. Wanda “Cognitive Radio Dinamic Spectrum Access Models (shared-use).” December 29 2010. http://trends-in-telecoms.blogspot.com/2010/12/cognitive-radio-dynamic-spectrum-access.html

[17] J.S. Mandeep, Nicholas “Design and X-Band Vivaldi Antenna.” July 2008, ED Online ID #19382. http://mwrf.com/Article/ArticleID/19382/19382.html

[18] Y. Hoon Chun, J. Hong, P.Bao, T.J. Jackson, M. J. Lancaster. “BST Varactor Tuned Bandstop Filter with Slotted Ground Structure.”IEEE 2008.

[19] M. Kazerooni, G. Rezai Rad, A. Cheldavi “Behavior Study of Simultaneously Defected Microstrip and Ground Structure (DMGS) in Planar Circuits,” March 2009

[20] E. Naglich, J. Lee, D. Peroulis, and W. J. Chappell “Tunable, Substrate Integrated, High Q Filter Cascade for High Isolation” IEEE 2010

[21] Y. Tawk, A. R. Albrecht, S. Hemmady, G. Balakrishnan, and C. G. Christodoulou, “Optically pumped frequency reconfigurable antenna design,” *IEEE Antennas and Wireless Propagation Letters,* vol. 9, pp. 280-283, 2010.

[22] G. H. Huff, and J. T. Bernhard, “Integration of packaged RF MEMS switches with radiation pattern reconfigurable square spiral microstrip antennas,” *IEEE Transactions on Antennas and Propagation,* vol. 54, no. 2, pp. 464-469, Feb.2006.

[23] A. Abdel-Rahman, A. R. Ali, S. Amari, and S.Omar, “Compact band pass filters using defected ground structures (DGS),” *IEEE MTT-S International Microwave Symposium,* pp. 1-4, 2005.

[24] I. Chang, and B. Lec, “Design of defected ground structures for harmonic control of active microstrip antenna,” *IEEE Antenna and Propagation Symposium,* pp. 852, 2002.

[25] Y. Tawk, and C. G. Christodoulou, "A new reconfigurable antenna design for cognitive radio," *IEEE Antennas and Wireless Propagation Letters,* vol.8, pp.1378-1381, 2009.

[26] Y. Tawk, M. Al-Husseini, S. Hemmady, A. R. Albrecht, G. Balakrishnan, and C. G. Christodoulou, "Implementation of a cognitive radio front-end using optically reconfigurable antennas," *International Conference on Electromagnetics in Advanced Applications (ICEAA),* , pp.294-297, Sept. 2010.

[27] M. E. Zamudio, Y. Tawk, J. Costantine, J. Kim,and C. G. Christodoulou, “ Integrated cognitive radio antenna using reconfigurable band pass filters,” 5th European Conference on Antennas and Propagation, Apr. 2011.

[28] Y.Sun, R. Xu,Y. Zhang, “A Design of the Novel Low pass Filter using Defected Ground Structure,” Asia Pacific Microwave Conference, 2005

[29] M. E. Zamudio, Y. Tawk, J. Costantine, S. E. Barbin, and C. G. Christodoulou "Reconfigurable Filter Embedded into an Antenna for UWB Cognitive Radio Environment" (ICEAA) conference, Sept. 2011.

[30] J. R. Kelly and P. S. Hall, "Reconfigurable slot antenna for cognitive radio application," in IEEE Antennas and Propagation Society International Symposium, 2009, pp. 1-4.

[31] M. Kazerooni1, A. Cheldavi1, and M. Kamarei2 "A Novel Bandpass Defected Microstrip Structure (DMS) Filter for Planar Circuits" PIERS Proceedings, Moscow, Russia, August 18-21, 2009.

[32] N. Symeon, G.E. ponchak, J. Papapolymerou, M.M. T. Jones, "*zeris*Conformal double exponentially tapered slot antenna (DETSA) on LCP for UWB applications ., IEEE trans, Antenna and Propation, vol. 54, pp. 1663-1669, Jun. 2006

[33] P. J. Gibson, "The Vivaldi aerial," Proceedings of the 9th European Microwave Conference, 1979, pp. 103-105.

[34] J. Peng, B. Wu, C.-H. Liang, and X.-F. Li. "Parameter Extraction For Microwave Coupled Resonator Filters Using Rational Model and Optimization" Progress In Electromagnetics Research M, Vol. 13, 109-119, 2010.

[35] Y. Tawk, J. Costantine, S. Hemmady, G. Balakrishnan, K. Avery, and C. G. Christodoulou, "Demonstration of a cognitive radio front-end using optically pumped reconfigurable antenna system (OPRAS)," IEEE Transactions on Antennas and Propagation, 2011 (Early Access).

APPENDIX A

A.1 VIVALDI ANTENNA MATLAB CODE

```
clear all;
Ysub = 40;
Xsub = 65;
n = 5;
T = 1.2;

W = 4.8;
a1 = (2/Xsub)*log((Ysub/2+W/2)/T+1);
a2 = (n/Xsub)*log(Ysub/2+W/2+1-W);

x = [0:Xsub/30:Xsub/2];
for ii = 1:length(x)
   y1(ii) = T*(exp(a1*x(ii))-1);
   if x(ii) <= Xsub/n
      y2(ii) = exp(a2*x(ii)) +W-1;
   else
      y2(ii) = Ysub/2+W/2;
   end
end

for kk = 1:length(x)-1
   xx(length(x)+kk) = x(length(x)-kk);
   y1(length(x)+kk) = y2(length(x)-kk);
end

for jj = 1:2*length(x)-1
   if jj <= length(x)
      xxn(jj) = x(jj);
   else
      xxn(jj) = xx(jj);
   end
end

plot(xxn,y1,'b');

fid1 = fopen('C:\Documents and Settings\Administrator\My
Documents\CST\Antenna_filter_int\TacLam+\data\tsa2.txt','wt');
for ii = 1:2*length(x)-1
   fprintf(fid1,'%6.2f\t %12.8f\n',xxn(ii),y1(ii));
end
fclose(fid1);
```

A.2 MATLAB GENERATED FIGURE

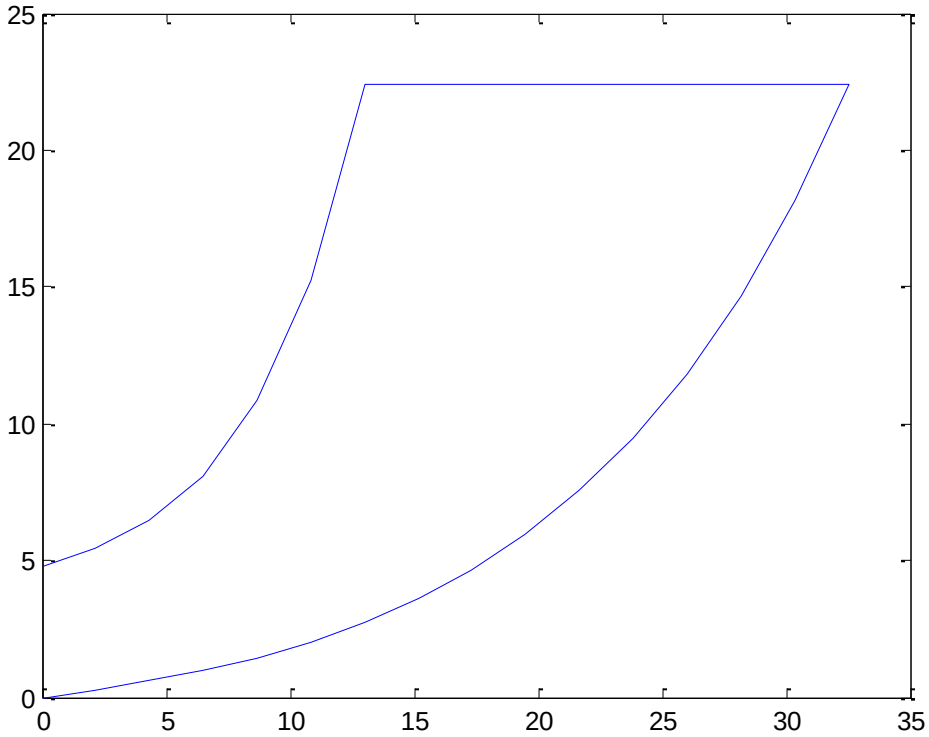

APPENDIX B

BIAS TEE SPECIFICATIONS

Model: BT-V000-HS

Description:..... ..... Bias Tee
Operating Frequency:..... ..... 0.5 – 20 GHz
Insertion Loss: .... 1.0 dB Max
VSWR:..... ..... 1.55:1 Max
Isolation DC to RF: .... 25dB Min
Bias Frequency Bandwidth..... ..... DC-50 MHz
RF Power:..... ..... 10W Max
Bias Voltage:..... ..... 50 Volts Max
Bias Current:..... ..... 220 mA Max
Bias DC Resistance:..... ..... 1.0 Ohms
RF Connector: .... SMA (f)
RF+DC Connector:..... ..... SMA (f)
Bias Connector: .... Solder Pin
Impedance:..... ..... 50 Ohms Nominal
Quality:..... ..... Best-Commercial-Grade

Environmental Ratings:

Temperature:..... {Operating: -55°C to +95°C} & {Storage: -60°C to +110°C}
Humidity: ..... MIL-STD-202F, Method 103B Cond. B (96 hours at 95% R.H.)
Shock: ..... MIL-STD-202F, Method 213B, Cond. B (75G, 6mSec)
Vibration: ..... MIL-STD-202F, Method 204D, Cond. B (.06" double amplitude, or 15G)
Altitude: ..... MIL-STD-202F, Method 105C, Cond. B (50,000 Feet)
Temp. Shock: ..... MIL-STD-202F, Method 107D, Cond. A (5 cycles)

Outline

[12.7mm]
[12.7mm]
DC+RF
RF
0.750"
[19.1mm]
0.500"
0.500"
SMA(F), 2 PLS
DC
GND

APPENDIX C

SMV 1405 VARACTOR SPECIFICATIONS

Features:

- High Q
- Low series resistance for low phase noise
- Designed for high volume commercial applications

Description:

The SMV1405 is a silicon abrupt junction varactor diode. The low resistance of this varactor makes it appropriate for high Q resonators in wireless system to frequencies beyond 2.5 GHz.

TYPICAL CAPACITANCE VALUES SMV1405

VR (V)	CT (pF)
0	2.67
0.5	2.12
1.0	1.84
1.5	1.7
2.0	1.55
2.5	1.44
3.0	1.34
4.0	1.25
5.0	1.25
10.0	0.95
20.0	0.77
30.0	0.63